AD_____

Award Number: DAMD17-01-1-0317

TITLE: Functional Analysis of Interactions Between 53BP1, BRCA1 and p53

PRINCIPAL INVESTIGATOR: Irene M. Ward, Ph.D.

CONTRACTING ORGANIZATION: Mayo Clinic and Foundation, Rochester
Rochester, Minnesota 55905

REPORT DATE: July 2003

TYPE OF REPORT: Annual Summary

PREPARED FOR: U.S. Army Medical Research and Materiel Command
Fort Detrick, Maryland 21702-5012

DISTRIBUTION STATEMENT: Approved for Public Release;
Distribution Unlimited

The views, opinions and/or findings contained in this report are those of the author(s) and should not be construed as an official Department of the Army position, policy or decision unless so designated by other documentation.

REPORT DOCUMENTATION PAGE

Form Approved
OMB No. 074-0188

1. AGENCY USE ONLY (Leave blank)	2. REPORT DATE	3. REPORT TYPE AND DATES COVERED
	July 2003	Annual Summary (1 Jul 2002 - 30 Jun 2003)

4. TITLE AND SUBTITLE
Functional Analysis of Interactions Between 53BP1, BRCA1 and p53

5. FUNDING NUMBERS
DAMD17-01-1-0317

6. AUTHOR(S)
Irene M. Ward, Ph.D.

7. PERFORMING ORGANIZATION NAME(S) AND ADDRESS(ES)
Mayo Clinic and Foundation, Rochester
Rochester, New York 55905

E-Mail: rappold.irene@mayo.edu

8. PERFORMING ORGANIZATION REPORT NUMBER

9. SPONSORING / MONITORING AGENCY NAME(S) AND ADDRESS(ES)
U.S. Army Medical Research and Materiel Command
Fort Detrick, Maryland 21702-5012

10. SPONSORING / MONITORING AGENCY REPORT NUMBER

11. SUPPLEMENTARY NOTES
Original contains color plates: All DTIC reproductions will be in black and white.

12a. DISTRIBUTION / AVAILABILITY STATEMENT
Approved for Public Release; Distribution Unlimited

12b. DISTRIBUTION CODE

13. ABSTRACT (Maximum 200 Words)

53BP1 has been suggested to play a role in DNA damage recognition and/or repair. We could show that upon exposure of cells to ionizing radiation, 53BP1 rapidly colocalizes with phosphorylated H2AX (g-H2AX) in megabase regions surrounding the sites of DNA strand breaks. The 53BP1 region required and sufficient for 53BP1 foci formation lies upstream of the 53BP1 C-terminus and binds to phosphorylated but not unphosphorylated H2AX in vitro. Moreover, phosphorylation of H2AX at S140 is critical for 53BP1 foci formation implying that a direct interaction between 53BP1 and g-H2AX is required for the accumulation of 53BP1 at DNA break sites. On the other hand, radiation-induced phosophorylation of the 53BP1 N-terminus by the ATM kinase is not essential for 53BP1 foci formation and occurs independently of 53BP1 redistribution. To further investigate the physiological role of 53BP1 we produced a targeted disruption of mouse 53BP1. 53BP1-deficient mice are radiation sensitive, growth retarded and immunodeficient. In addition, 53BP1-/- mice show a higher incidence of developing thymic lymphomas suggesting that 53BP1 plays a role in tumor suppression.

14. SUBJECT TERMS
DNA damage, DNA repair, tumorigenesis, genomic stabiltiy

15. NUMBER OF PAGES
25

16. PRICE CODE

17. SECURITY CLASSIFICATION OF REPORT	18. SECURITY CLASSIFICATION OF THIS PAGE	19. SECURITY CLASSIFICATION OF ABSTRACT	20. LIMITATION OF ABSTRACT
Unclassified	Unclassified	Unclassified	Unlimited

Table of Contents

INTRODUCTION

Defects in recognition and repair of DNA damage may be the decisive step in the transformation of a healthy cell into a tumor cell. 53BP1 has been suggested to participate in the DNA damage response pathway based on its C-terminal tandem BRCT (BRCA1 C-terminal) domain and the observation that 53BP1 relocalizes to discrete nuclear foci upon exposure of cells to ionizing radiation (Anderson et al., 2001; Rappold et al., 2001; Schultz et al., 2000; Xia et al., 2000).

To obtain insight into the function of this protein we asked whether 53BP1 interacts with p53, BRCA1 or other proteins known to be involved in the DNA damage response. Although the results demonstrated that 53BP1 participates early in the DNA damage pathway its function remained elusive. We therefore created a 53BP1-deficient mouse model and are investigating whether loss of 53BP1 function leads to defects in DNA repair and/or cell cycle checkpoint control and whether 53BP1 plays a role in maintaining genomic stability and tumor suppression.

BODY

As outlined in the *Statement of Work*, the first two years of the grant proposal focussed on the interaction of 53BP1 with the tumor suppressors BRCA1 and p53. We had produced monoclonal and polyclonal antibodies towards 53BP1 and demonstrated that 53BP1 colocalizes and interacts with BRCA1 several hours after exposure of cells to ionizing radiation. This interaction occurs at sites of DNA double strand breaks as shown by co-immunostaining with an antibody towards the activated form of H2AX, a histone H2A variant that becomes phosphorylated at areas of DNA stand breaks (described in previous annual report and (Rappold et al., 2001)). In contrast, the interaction of 53BP1 and p53 does not depend on DNA damage. To characterize the 53BP1 domains that mediate the recruitment of 53BP1 to sites of DNA strand breaks we generated a series of HA-tagged 53BP1 full-length and deletion mutants and studied the IR-induced relocalization of these fusion proteins in transiently transfected U2OS cells. We could

show that a region upstream of the tandem BRCT domains is required and sufficient for the accumulation of 53BP1 to DNA strand breaks (Fig. 1).

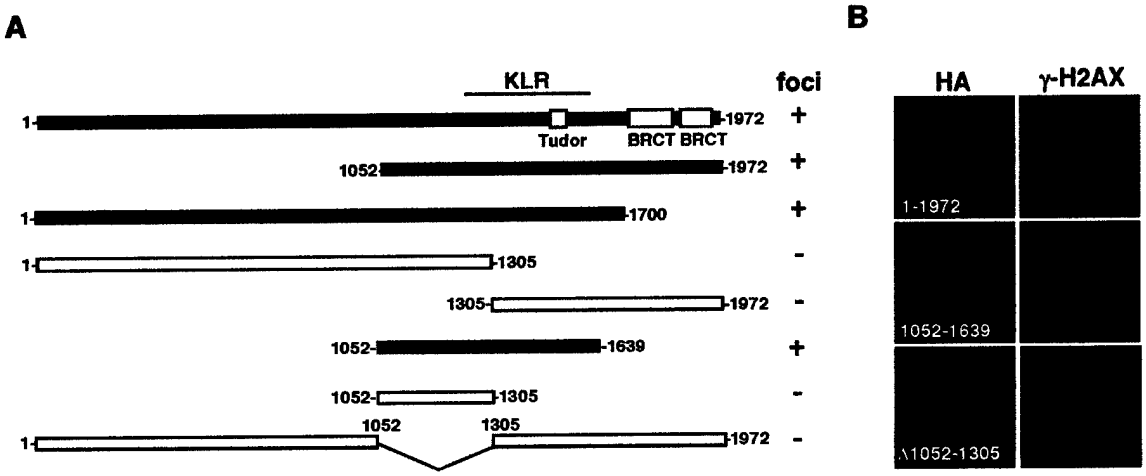

Fig.1: A region upstream of the BRCT domains is required and sufficient for damage-induced focus localization of 53BP1. **A**: Schematic diagram of the wild-type or mutant 53BP1 constructs that were N-terminally fused to a 3xNLS and an HA-tag. Their ability to form damage-induced foci is indicated by a (+). KLR refers to the kinetochore localization region. **B**: U20S cells transiently expressing the HA-53BP1 constructs were irradiated with 1 Gy and immunostained 1 h later with anti- HA and anti-γ-H2AX antibodies.

Interestingly, this region also binds to phosphorylated but not unphosphorylated H2AX *in vitro* (Fig.2), suggesting that phosphorylated H2AX keeps 53BP1 in the vicinity of DNA lesions.

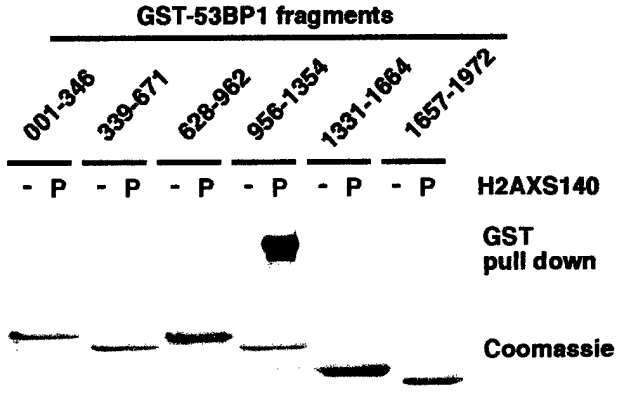

Fig.2: The 53BP1 region required for focus formation binds to phosphorylated H2AX *in vitro*. GST-53BP1 fragments, encoding different regions of 53BP1 as indicated, were incubated with an immobilized C-terminal H2AX peptide that was either phosphorylated or not at S140. Pulled down proteins were identified by SDS PAGE followed by immunoblotting with anti-GST antibodies.

Moreover, using H2AX-deficient cells reconstituted with wild-type or a phosphorylation-deficient mutant of H2AX we could show that H2AX phosphorylation at serine 140 is critical for 53BP1 accumulation at sites of DNA strand breaks (Fig.3 and Ward et al., 2003a, appendix).

Fig.3: 53BP1 focus formation requires binding to phosphorylated S140 of H2AX.
H2AX-/- ES cells were transiently transfected with either HA-tagged wild-type H2AX (H2AXwt) or a S140A phosphomutant. 53BP1 foci formation was assessed by IF 1 h after exposure of cells to 1 Gy of IR.

Since 53BP1 becomes hyperphosphorylated in response to DNA damage, we wondered whether 53BP1 phosphorylation is required for the interaction with phospho-H2AX. We mapped four *in vitro* phosphorylation sites, raised phospho-specific antibodies against these sites and showed that at least two of them (S25 and S29) are phosphorylated *in vivo* by ATM, the kinase mutated in cancer prone ataxia telangiectasia patients. 53BP1 mutants that lack all four phosphorylation sites were still able to relocate to γ-H2AX containing foci in response to ionizing radiation, suggesting that 53BP1 phosphorylation is not required for 53BP1 accumulation. In addition, 53BP1 mutants that lack the region required for 53BP1 accumulation and do not relocate to foci in response to ionizing radiation can still be phosphorylated (Fig. 4 and Ward et al., 2003a, appendix). Therefore, 53BP1 phosphorylation and 53BP1 relocalization appear to be regulated independently.

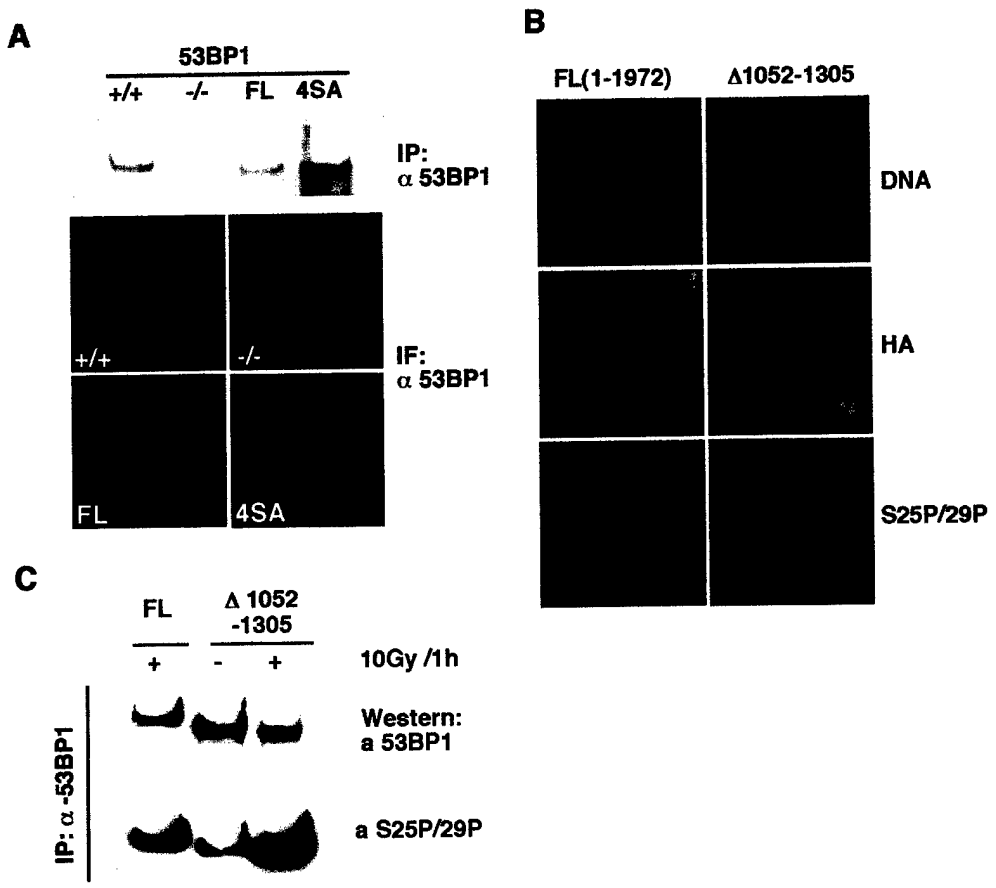

Fig.4: Damage-induced phopshorylation of 53BP1 occurs independent of 53BP1 foci formation. **A**: ATM-dependent 53BP1 phosphorylation is not required for 53BP1 foci formation. HA-tagged full length 53BP1 (FL) or a phosphorylation-deficient mutant of 53BP1 (4SA) were stable expressed in 53BP1-deficient embryonic cells. 53BP1 expression levels were assessed by immunoprecipitation. 53BP1 foci formation was analysed by IF 1 h after 1 Gy of IR. **B**: 53BP1 foci formation is not required for ATM-dependent 53BP1 phsophorylation. 53BP1-deficient embryonic cells were transiently transfected with HA-tagged full length 53BP1 or a deletion mutant lacking part of the focus formation region. 53BP1 localisation and ATM-dependent phosphorylation was analyzed 1 h after 1 Gy of IR by costaining with anti-HA antibody and anti-phospho-53BP1 antiserum (anti-25P/29P). **C**: An aliquot of the transfected cells was either mock treated or irradiated with 10 Gy . 53BP1 was immnoprecipitated from cell lysates and 53BP1 phsophorylation was analyzed by immunoblotting with the phsopho-specific anti-S25P/S29P antibody.

To examine the pysiological relevance of the observed interactions between 53BP1, BRCA1 and p53 we generated a 53BP1-deficient mouse model (for details see Ward et al., 2003b, appendix). Mice that lack 53BP1 were growth retarded, radiation sensitive and immunodeficient (Ward et al., 2003b). Immunofluorescence staining of BRCA1 on mouse embryonic fibroblasts (MEFs) derived from 53BP1-/- and 53BP1+/+ littermates demonstrated that 53BP1 is not required for radiation-induced relocation of BRCA1 to

DNA strand breaks. Initial experiments that suggested impaired BRCA1 foci formation in the absence of 53BP1 turned out to be a staining artifact. To check whether 53BP1 transduces a DNA damage signal to p53, we compared irradiation-induced p53 stabilization in 53BP1+/+ and 53BP1-/- thymocytes and MEFs. Although p53 levels increased in both 53BP1 wild-type and 53BP1-deficient cells upon irradiation, in some experiments we observed a reduced and/or delayed p53 response in the absence of 53BP1 suggesting that 53BP1 may have a subtle effect on p53 regulation.

To explore whether 53BP1 is involved n the maintenance of genomic stability we looked for chromosomal aberrations in 53BP1-deficient MEFs. 53BP1-/- cells showed a tendency to aneuploidy and tetraploidy when compared to 53BP1 wild-type cells. Genomic instability is a hallmark and prerequisite of cancer. Notably, about 8% of the 53BP1-deficient mice developed thymic lymphomas within 4 and 7 months of age (Fig.5). In contrast, none of the 53BP1+/+ and 53BP1+/- littermates developed any tumors within the first year of life (Ward et al., 2003b).

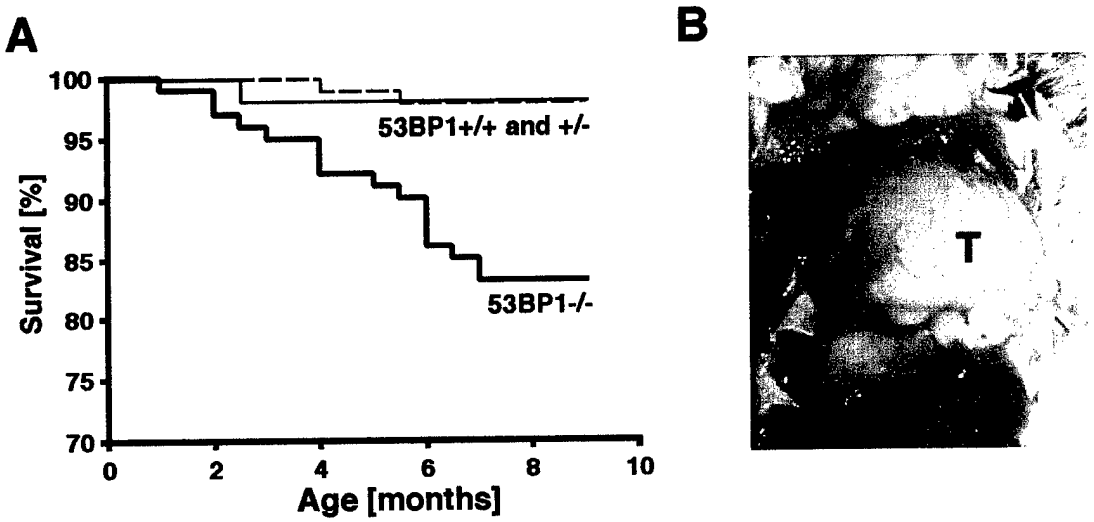

Fig.5: 53BP1 -/-mice are tumor prone. **A**: Overall survival of 53BP1+/+ (n=54), 53BP1+/- (n=97) and 53BP1-/- (n=101) over the course of 10 months. **B**: Massive thymic lymphoma (T) in a 4-months old 53BP1-/- mouse.

Since the genetic background of a given mouse strain greatly influences tumor susceptibility as well as tumor type we are currently back-crossing our 53BP1-deficient

mice into a BALB/c background. We are especially interested to examine whether 53BP1-deficient mice show a higher incidence of breast and/or ovarian cancers when compared to 53BP1 wild-type mice. In addition, we are crossing 53BP1 heterozygous mice with p53 heterozygous mice of the same mixed background to investigate how both proteins contribute to tumor formation.

Immunohistochemical staining of a breast cancer tissue array showed that 53BP1 is overexpressed in a number of breast cancers. We will soon receive additional breast cancer as well as ovarian cancer arrays from in house sources to extend our screening.

KEY RESEARCH ACCOMPLISHMENTS

We have shown that:

- 53BP1 participates together with BRCA1 and p53 in the DNA damage response
- 53BP1 rapidly accumulates at sites of DNA strand breaks in response to genotoxic stress
- 53BP1 accumulation is mediated by a direct interaction with phospho-H2AX
- 53BP1-deficient mice are radiation sensitive, growth retarded and immunodeficient
- 53BP1-deficient mice have a higher incidence of developing thymic lymphomas
- 53BP1 is overexpressed in a subset of breast cancer tissues

REPORTABLE OUTCOMES

Manuscripts:

Rappold, I.M., Iwabuchi, K., Date, T. and Chen, J. (2001) Tumor suppressor p53 binding protein 1 (53BP1) is involved in DNA damage-signaling pathways. *J Cell Biol*, **153**,

Ward, I.M., Wu, X. and Chen, J. (2001) Threonine 68 of Chk2 is phosphorylated at sites of DNA strand breaks. *J Biol Chem*, **276**, 47755-8)

Ward, I.M. and Chen, J. (2001) Histone H2AX is phosphorylated in an ATR-dependent manner in response to replicational stress. *J Biol Chem*, **276**, 47759-62.

Fernandez-Capetillo, O., Chen, H.T., Celeste, A., **Ward, I.**, Romanienko, P.J., Morales, J.C., Naka, K., Xia, Z., Camerini-Otero, R.D., Motoyama, N., Carpenter, P.B., Bonner, W.M., Chen, J. and Nussenzweig, A. (2002) DNA damage-induced G2-M checkpoint activation by histone H2AX and 53BP1. *Nat Cell Biol*, **4**, 993-7.

Ward, I.M., Minn, K., Jorda, K.G. and Chen, J. (2003a) Accumulation of checkpoint protein 53BP1 at DNA breaks involves its binding to phosphorylated histone H2AX. *J Biol Chem*, **278**, 19579-82.

Ward, I.M., Minn, K., van Deursen, J. and Chen, J. (2003b) p53 Binding protein 53BP1 is required for DNA damage responses and tumor suppression in mice. *Mol Cell Biol*, **23**, 2556-63.

Animal model:

Generation of a 53BP1-deficient mouse model

Development of cell lines:

Establishment of immortal 53BP1-deficient and 53BP1-wildtype mouse embryonic cell lines

CONCLUSIONS

Our data demonstrate that 53BP1 plays a role early in the DNA damage response. It relocalizes to sites of DNA double strand breaks and binds to phosphorylated histone H2AX upon exposure of cells to ionizing radiation. The region that binds to phosphorylated H2AX resides within the region required for 53BP1 foci formation upstream of the C-terminal BRCT domains. Although 53BP1 becomes hyperphosphorylated by ATM in response to ionizing radiation, phosphorylation can occur in the absence of 53BP1 foci formation suggesting that both events are regulated independently. Knock out mice that lack 53BP1 protein exhibit an increased sensitivity to ionizing radiation and show a higher incidence of developing thymic lymphomas suggesting that 53BP1 plays a role in tumor suppression. Thus, unraveling 53BP1 function and the underlying molecular mechanism will contribute to our understanding of tumorigenesis.

REFERENCES

Anderson, L., Henderson, C. and Adachi, Y. (2001) Phosphorylation and rapid relocalization of 53BP1 to nuclear foci upon DNA damage. *Mol Cell Biol*, **21**, 1719-29.

Rappold, I., Iwabuchi, K., Date, T. and Chen, J. (2001) Tumor Suppressor p53 Binding Protein 1 (53BP1) Is Involved in DNA Damage-signaling Pathways. *J Cell Biol*, **153**, 613-20.

Schultz, L.B., Chehab, N.H., Malikzay, A. and Halazonetis, T.D. (2000) p53 Binding Protein 1 (53BP1) Is an Early Participant in the Cellular Response to DNA Double-Strand Breaks. *J Cell Biol*, **151**, 1381-1390.

Ward, I.M., Minn, K., Jorda, K.G. and Chen, J. (2003a) Accumulation of checkpoint protein 53BP1 at DNA breaks involves its binding to phosphorylated histone H2AX. *J Biol Chem*, **278**, 19579-82.

Ward, I.M., Minn, K., Van Deursen, J. and Chen, J. (2003b) p53 Binding Protein 53BP1 Is Required for DNA Damage Responses and Tumor Suppression in Mice. *Mol Cell Biol*, **23**, 2556-63.

Xia, Z., Morales, J.C., Dunphy, W.G. and Carpenter, P.B. (2000) Negative cell cycle regulation and DNA-damage inducible phosphorylation of the BRCT protein 53BP1. *J Biol Chem*.

APPENDICES

Ward, I.M., Minn, K., Jorda, K.G. and Chen, J. (2003a) Accumulation of checkpoint protein 53BP1 at DNA breaks involves its binding to phosphorylated histone H2AX. *J Biol Chem*, **278**, 19579-82.

Ward, I.M., Minn, K., van Deursen, J. and Chen, J. (2003b) p53 Binding protein 53BP1 is required for DNA damage responses and tumor suppression in mice. *Mol Cell Biol*, **23**, 2556-63.

Accelerated Publication

THE JOURNAL OF BIOLOGICAL CHEMISTRY
Vol. 278, No. 22, Issue of May 30, pp. 19579–19582, 2003

Accumulation of Checkpoint Protein 53BP1 at DNA Breaks Involves Its Binding to Phosphorylated Histone H2AX*

Received for publication, March 14, 2003,
and in revised form, April 15, 2003
Published, JBC Papers in Press, April 15, 2003,
DOI 10.1074/jbc.C300117200

Irene M. Ward‡§, Kay Minn‡, Katherine G. Jorda¶, and Junjie Chen‡‖

From the ‡Department of Oncology, Mayo Clinic and Foundation, Rochester, Minnesota 55905 and the ¶Division of Oncology, Columbia University, New York, New York 10032

53BP1 participates in the cellular response to DNA damage. Like many proteins involved in the DNA damage response, 53BP1 becomes hyperphosphorylated after radiation and colocalizes with phosphorylated H2AX in megabase regions surrounding the sites of DNA strand breaks. However, it is not yet clear whether the phosphorylation status of 53BP1 determines its localization or vice versa. In this study we mapped a region upstream of the 53BP1 C terminus that is required and sufficient for the recruitment of 53BP1 to these DNA break areas. *In vitro* assays revealed that this region binds to phosphorylated but not unphosphorylated H2AX. Moreover, using H2AX-deficient cells reconstituted with wild-type or a phosphorylation-deficient mutant of H2AX, we have shown that phosphorylation of H2AX at serine 140 is critical for efficient 53BP1 foci formation, implying that a direct interaction between 53BP1 and phosphorylated H2AX is required for the accumulation of 53BP1 at DNA break sites. On the other hand, radiation-induced phosphorylation of the 53BP1 N terminus by the ATM (ataxia-telangiectasia mutated) kinase is not essential for 53BP1 foci formation and takes place independently of 53BP1 redistribution. Thus, these two damage-induced events, hyperphosphorylation and relocalization of 53BP1, occur independently in the cell.

The DNA of eukaryotic cells is constantly exposed to endogenous and exogenous DNA-damaging agents. To prevent the accumulation of genomic damage and avert cellular dysfunction, cells have evolved complex response mechanisms. 53BP1 was initially identified as a protein that binds to the central DNA binding domain of p53 and enhances p53-mediated transcriptional activation (1, 2). In response to genotoxic stress, 53BP1 rapidly redistributes from a diffuse nuclear localization into distinct nuclear foci suggesting that 53BP1 is involved in the DNA damage response (3–6). Moreover the C terminus of 53BP1 contains two BRCT domains, a motif found in a number of proteins implicated in various aspects of cell cycle control, recombination, and DNA repair (7, 8). Subsequent studies have shown that 53BP1 becomes hyperphosphorylated in response to ionizing radiation (IR)[1] and colocalizes with phosphorylated histone H2AX (γ-H2AX) at the sites of DNA lesions (3, 4). Other proteins known to be involved in the DNA damage signaling pathway (*i.e.* BRCA1, Rad51, NBS1, and TopoBP1) were also found to colocalize with 53BP1 in these inducible foci (3, 4, 6, 9). Direct evidence for an important role of 53BP1 in the DNA damage response came recently from studies using 53BP1-deficient cells. Human cell lines treated with specific small interfering RNA to silence 53BP1 expression exhibited a defect in the intra-S phase checkpoint and, at low IR doses, a partial defect in the G_2-M checkpoint (10–12). Moreover 53BP1-deficient mice are hypersensitive to ionizing radiation and show an increased incidence of developing thymic lymphomas (13). Several lines of evidence suggest that 53BP1 is a substrate of ATM, the kinase mutated in the human disease ataxia-telangiectasia, and is involved in the phosphorylation of various ATM substrates (3, 6, 10).

Despite this recent progress made toward 53BP1 function little is known about the initial activation of 53BP1. Recruitment of 53BP1 to γ-H2AX foci seems to be a crucial step. H2AX-deficient cells lack normal 53BP1 foci formation and, like 53BP1-deficent cells, manifest a G_2-M checkpoint defect after exposure to low doses of ionizing radiation (12). Moreover, H2AX−/− mice show a radiation sensitivity similar to 53BP1−/− mice (14). In this study we mapped the region required for 53BP1 foci formation in response to DNA damage. We show that a region upstream of the BRCT motifs is sufficient for 53BP1 foci formation and that this region interacts directly with phosphorylated H2AX. Using H2AX-deficient cells retransfected with either wild-type H2AX or an H2AX phosphomutant we confirm that phosphorylation of H2AX at Ser-140 is required for 53BP1 accumulation at DNA break areas. In contrast, radiation-induced phosphorylation of 53BP1 by ATM is not essential for the recruitment of 53BP1 to foci and occurs independently.

EXPERIMENTAL PROCEDURES

Plasmid Constructs and Transfection—53BP1 deletion mutants were generated by inserting stop codons and/or restriction sites at various positions into pCMH6K 53BP1 (2) using the QuikChange site-directed mutagenesis kit (Stratagene). A 3×NLS (nuclear localization sequence) was inserted into the *NheI* site upstream of the N-terminal hemagglutinin (HA) and His_6 tags. U2OS cells were transfected using FuGENE 6 (Roche Applied Science) according to the manufacturer's instructions. H2AX was PCR-amplified from human genomic DNA and inserted between the HA tag and an internal ribosomal entry site fused to the puromycin gene of a modified pcDNA3 vector. The H2AX phosphomutant was generated by replacing Ser-140 of H2AX with an alanine using the QuikChange mutagenesis kit (Stratagene). H2AX-deficient embry-

* This work was supported by grants from the National Institutes of Health, Breast Cancer Research Foundation, and Prospect Creek Foundation. The costs of publication of this article were defrayed in part by the payment of page charges. This article must therefore be hereby marked "*advertisement*" in accordance with 18 U.S.C. Section 1734 solely to indicate this fact.

§ Supported by a postdoctoral fellowship from the Department of Defense breast cancer research program.

‖ Recipient of a Department of Defense breast cancer career development award. To whom correspondence should be addressed. Tel.: 507-538-1545; Fax: 507-284-3906; E-mail: Chen.junjie@mayo.edu.

[1] The abbreviations used are: IR, ionizing radiation; γ-H2AX, phosphorylated histone H2AX; ATM, ataxia-telangiectasia mutated; NLS, nuclear localization sequence; HA, hemagglutinin; ES, embryonic stem; KLH, keyhole limpet hemocyanin; Gy, gray(s); GST, glutathione *S*-transferase; aa, amino acid(s); IF, immunofluorescence; BRCT, BRCA1 C terminus.

onic stem (ES) cells (provided by C. Bassing, Ref. 15) were transfected by electroporation.

Antibodies—Anti-S6P, anti-S25P/29P, and anti-S784P specific antibodies were generated by coupling synthetic 53BP1 peptides (S6P, CDPTG(P)SQLD; S25P/29P, CIED(P)SQPE(P)SQVLEDD; S784P, CSD(P)SQSWEDI where (P)S represents phosphoserine) to KLH using Imject maleimide-activated mcKLH (Pierce) prior to immunizing rabbits (Cocalico Biological). The antibodies were affinity-purified on agarose columns coupled with the non-phosphorylated or phosphorylated peptide (SulfoLink Coupling Gel, Pierce). Anti-53BP1 and anti-γ-H2AX antibodies were generated as described previously (3). Monoclonal antibody HA11 specific for HA was purchased from BabCO Berkeley Antibody Co. Anti-ATM antibody Ab3 was purchased from Oncogene Research Products.

Immunofluorescence Staining, Immunoblots, and Immunoprecipitation—Cells grown on coverslips were fixed with 3% paraformaldehyde 1 h after exposure to 0 or 1 Gy of IR. After permeabilization with 0.5% Triton X-100, cells were blocked with 5% goat serum and incubated successively with the primary and secondary antibodies, each for 25 min at 37 °C. In case of DNase or RNase treatment, cells were irradiated, permeabilized with 0.5% Triton X-100 for 3 min, and incubated with either DNase I (10 units/ml) or RNase A (50 μg/ml) in phosphate-buffered saline plus calcium and magnesium for 30 min at 37 °C prior to fixation with 3% paraformaldehyde. Immunoprecipitation and immunoblot assays were done as described previously (3).

ATM Kinase Assays—ATM was precipitated from K562 cells, and aliquots of the ATM-protein A-Sepharose immunocomplex were resuspended in 25 μl of kinase buffer (10 mM Hepes (pH 7.4), 50 mM NaCl, 10 mM $MgCl_2$, 10 mM $MnCl_2$, 1 mM dithiothreitol, 10 nM ATP). ATM kinase reactions were carried out at 30 °C for 20 min with 10 μCi of [γ-^{32}P]ATP and 1 μg of 53BP1 GST fusion proteins.

GST Pull-down Assays—GST pull-down experiments were performed by incubating 3 μg of various GST-labeled 53BP1 fragments with C-terminal H2AX peptide that was either phosphorylated or unphosphorylated at Ser-140 (CKATQA(P)SQEY) and had been immobilized on SulfoLink Coupling Gel (Pierce). Bound GST proteins were isolated by incubating the mixture for 1 h at 4 °C in 200 μl of NETN buffer (150 mM NaCl, 1 mM EDTA, 20 mM Tris (pH 8), 0.5% Nonidet P-40), washing five times with NETN, eluting the proteins with 2× Laemmli buffer, separating them by SDS-PAGE, and immunoblotting with horseradish peroxidase-conjugated anti-GST (B-14, Santa Cruz Biotechnology).

Generation of 53BP1-deficient Embryonic Cells—A 53BP1-deficient embryonic cell line was derived from 53BP1−/− blastocysts using a standard procedure. The generation of 53BP1-deficient mice is described in Ref. 13.

RESULTS

A Region Upstream of the Tandem BRCT Motif Is Required and Sufficient for 53BP1 Foci Formation—53BP1 is a large 1972-aa nuclear protein with a C-terminal tandem BRCT motif. Upstream of the BRCT repeats resides a bipartite nuclear localization signal (predictNLS, Ref. 16) and a tudor domain (RPS-BLAST, Ref. 17), a motif found in several RNA-binding proteins. In response to IR, 53BP1 rapidly redistributes to distinct nuclear foci that colocalize with γ-H2AX (3, 4, 6). Treatment of irradiated cells with DNase, but not RNase, completely abolished 53BP1 and γ-H2AX foci formation confirming that these foci localize to DNA (Fig. 1*A*).

To determine the minimal region required for the recruitment of 53BP1 to damage-induced foci, we generated various HA-tagged 53BP1 deletion mutants and examined their distribution in transiently transfected U2OS cells (Fig. 1, *B* and *C*, and data not shown). A 3×NLS motif fused to the N terminus of 53BP1 ensured nuclear expression of the various constructs. Truncation of the 53BP1 N terminus (Δ1–1052) or the BRCT domains (Δ1700–1972) did not affect 53BP1 foci formation as assessed by IF 1 h after exposure to 1 Gy of IR (Fig. 1*C*). However, increasing C-terminal deletions (Δ1305–1972 and Δ1052–1972) or deletion of a region upstream of the tandem BRCT motifs (Δ1052–1305) abolished 53BP1 foci formation (Fig. 2, *B* and *C*, and data not shown). Moreover a 53BP1 construct expressing residues 1052–1639 including the tudor

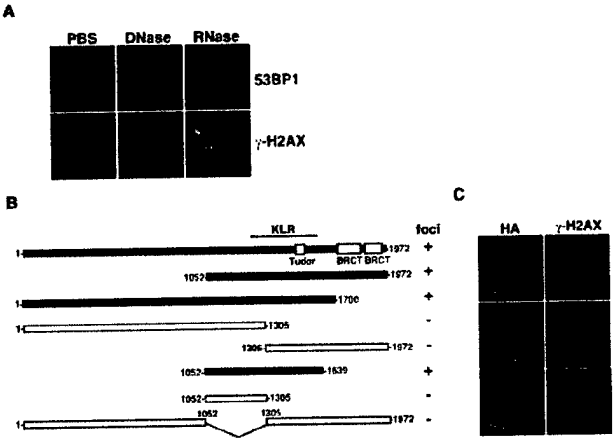

FIG. 1. **A region upstream of the BRCT domains is required and sufficient for damage-induced focus localization of 53BP1.** *A*, DNase but not RNase treatment abolishes 53BP1 and γ-H2AX foci formation in response to 1 Gy of IR. *B*, schematic diagram of the wild-type or mutant 53BP1 constructs that were N-terminally fused to a 3×NLS and an HA tag. Their abilities to form damage-induced foci is indicated by a +. *KLR* refers to the kinetochore localization region. *C*, U20S cells transiently expressing the HA-53BP1 constructs were irradiated with 1 Gy and immunostained 1 h later with anti-HA and anti-γ-H2AX antibodies. *PBS*, phosphate-buffered saline.

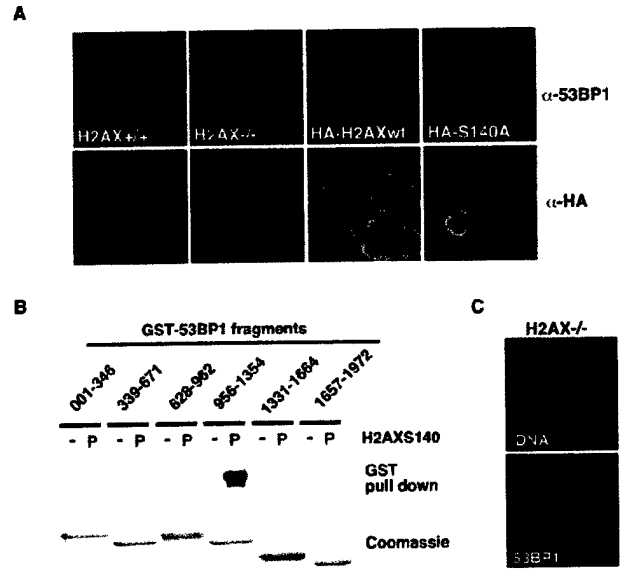

FIG. 2. **53BP1 foci formation requires its binding to phosphorylated Ser-140 of H2AX.** *A*, H2AX−/− ES cells were transiently transfected with either HA-tagged wild-type H2AX (*HA-H2AXwt*) or a S140A phosphorylation-deficient mutant (*HA-S140A*). 53BP1 foci formation was assessed by IF 1 h after exposure of cells to 1 Gy of IR. *B*, GST-53BP1 fragments, encoding different regions of 53BP1 as indicated, were incubated with immobilized C-terminal H2AX peptide that was either phosphorylated (*P*) or not at Ser-140. Pulled down proteins were separated by SDS-PAGE followed by immunoblotting with anti-GST antibodies. The addition of similar amounts of various GST proteins was verified by SDS-PAGE and Coomassie Blue staining. *C*, H2AX−/− cells were stained with anti-53BP1 antibodies and 4,6-diamidino-2-phenylindole, and mitotic cells were analyzed for kinetochore localization of 53BP1.

domain was found to be sufficient for 53BP1 foci formation (Fig. 1, *B* and *C*) suggesting that the domain required for foci formation is contained within this region.

53BP1 Focus Localization Region Interacts Directly with γ-H2AX—H2AX-deficient cells show greatly reduced 53BP1 foci formation implying that H2AX is involved in the recruit-

ment of 53BP1 to radiation-induced foci (14). H2AX becomes phosphorylated at a conserved C-terminal SQ site upon exposure of cells to ionizing radiation (18). Phosphorylation of H2AX at Ser-140 is impaired in ATM-deficient cells suggesting that this site is dominantly phosphorylated by ATM (12). To analyze whether phosphorylation of H2AX at Ser-140 is required for 53BP1 redistribution we transiently expressed wild-type H2AX or a S140A phosphomutant in H2AX-deficient ES cells and assessed 53BP1 foci formation. As shown in Fig. 2*A*, expression of wild-type H2AX reconstituted 53BP1 foci formation in response to IR. In marked contrast, expression of the H2AX S140A phosphomutant was insufficient to induce 53BP1 accumulation at the sites of DNA strand breaks.

We had shown earlier that phosphorylated H2AX co-immunoprecipitates with 53BP1 upon exposure of cells to DNA damage (3). To determine whether the region required for 53BP1 focus localization interacts directly with γ-H2AX, we used an *in vitro* pull-down assay. Six different 53BP1 GST fragments spanning the entire 53BP1 protein were incubated with immobilized C-terminal H2AX peptide that was either phosphorylated or non-phosphorylated at Ser-140. Only 53BP1 fragment 956–1354, which overlaps with the mapped focus localization region, showed strong interaction with the phosphorylated H2AX peptide (Fig. 2*B*). As a control, no binding was detected to the non-phosphorylated peptide bearing identical sequence (Fig. 2*B*).

Since H2AX directs 53BP1 accumulation in response to DNA damage, we asked whether H2AX is also required for the kinetochore localization of 53BP1 in mitotic cells (19). As shown in Fig. 2*C*, 53BP1 can be readily detected at the kinetochores in H2AX-deficient mitotic cells suggesting that the kinetochore localization of 53BP1 is not mediated by phospho-H2AX.

Phosphorylation of 53BP1 Is Not Required for Foci Formation—We had previously demonstrated that 53BP1 becomes hyperphosphorylated in response to IR, and three regions at the N terminus of 53BP1 were found to be phosphorylated by ATM *in vitro* (3). To map the phosphorylation sites we designed a series of GST fusion peptides containing one or two ATM binding motifs (SQ or TQ sites). ATM kinase assays using these purified GST fusion proteins as substrates, and ATM kinase immunoprecipitated from either K562 lysates (containing wild-type ATM) or ATM-deficient GM03189D lysates revealed peptides aa 1–12, aa 18–37, and aa 778–791 as putative ATM substrates (Fig. 3*A*). To examine whether the respective SQ sites become phosphorylated *in vivo*, we raised polyclonal antibodies against phosphorylated Ser-6 (anti-S6P), phosphorylated Ser-25 and Ser-29 (anti-S25P/29P), and phosphorylated Ser-784 (anti-S784P). All affinity-purified antisera recognized 53BP1 in irradiated cells but not in untreated controls when assessed by immunofluorescence analysis (data not shown). In addition, anti-53BP1 S25P/29P antibodies detected 53BP1 from irradiated ATM wild-type but not ATM-deficient cells by Western blot analyses (Fig. 3*B*). Pretreatment with λ-phosphatase abolished the antibody binding further validating that anti-53BP1 S25P/29P specifically recognizes the phosphorylated form of 53BP1 (Fig. 3*B*).

To test whether phosphorylation of 53BP1 is required for the recruitment of 53BP1 to sites of DNA lesions, we generated a phosphorylation-deficient mutant (53BP1 4SA) by mutating the mapped ATM target sites (Ser-6, Ser-25/Ser-29, and Ser-784) to alanines. 53BP1−/− embryonic cells transfected with this phosphomutant showed normal 53BP1 foci formation in response to IR (Fig. 3*C*), indicating that ATM-dependent phosphorylation of 53BP1 is not required for recruitment to or retention of 53BP1 at DNA break sites.

Phosphorylation of 53BP1 might occur at the break areas. To test this possibility, we transiently transfected 53BP1-deficient embryonic cells with the HA-tagged mutant that lacks part of the 53BP1 focus localization region (Δ1052–1305) and remains a diffuse nuclear localization upon exposure of cells to IR. Co-immunostaining with anti-HA and anti-53BP1 S25P/29P antibodies revealed that ATM-dependent 53BP1 phosphorylation does not require 53BP1 foci formation (Fig. 3*D*). Immunoprecipitation assays confirmed that 53BP1 Δ1052–1305 becomes readily phosphorylated at Ser-25/Ser-29 in response to IR (Fig. 3*E*). These findings are consistent with a recent report describing phosphorylation of 53BP1 Ser-25 in H2AX-deficient cells (12). Taken together, these results suggest that 53BP1 focus localization and ATM-dependent phosphorylation of 53BP1 are regulated independently.

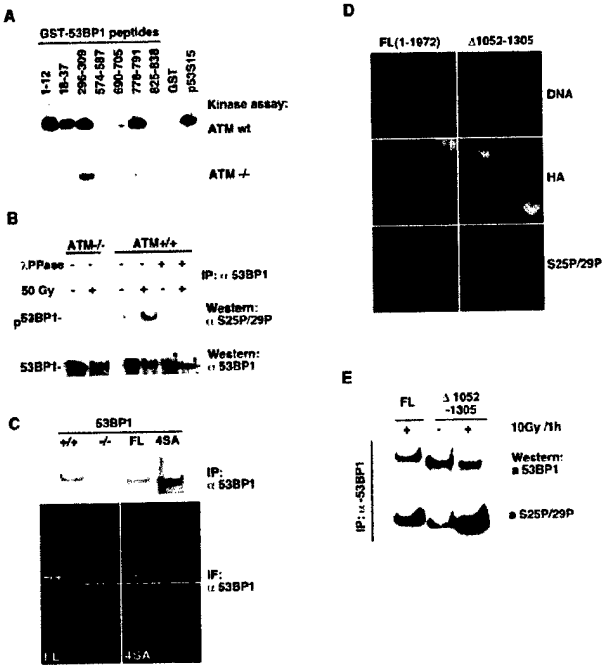

FIG. 3. **Damage-induced phosphorylation of 53BP1 occurs independently of 53BP1 foci formation.** *A*, *in vitro* mapping of potential ATM phosphorylation sites. ATM kinase assays were performed using ATM kinase immunoprecipitated from K562 lysates (ATM wild type) or GM03189D lysates (ATM-deficient) and GST fusion peptides containing one or two SQ or TQ sites of 53BP1. GST or GST fusion protein containing 14 amino acids surrounding the Ser-15 of p53 (*p53S15*) were used as negative and positive controls, respectively. *B*, 53BP1 is phosphorylated *in vivo* following IR. 293T cells containing wild-type ATM and ATM-deficient GM03189D cells were mock-treated or irradiated (50 Gy). After 1 h, whole cell lysates were immunoprecipitated with anti-53BP1 antibody. Duplicate samples were treated with or without λ-phosphatase (*λPPase*). Western blots were performed with anti-53BP1 or an anti-phospho-53BP1 antiserum raised against the phosphoserines 25/29 of 53BP1. *C*, ATM-dependent 53BP1 phosphorylation is not required for 53BP1 foci formation. HA-tagged full-length 53BP1 (*FL*) or a phosphorylation-deficient mutant of 53BP1 (*4SA*) were stably expressed in 53BP1-deficient embryonic cells. 53BP1 expression levels were assessed by immunoprecipitation. 53BP1 foci formation was analyzed by IF 1 h after 1 Gy of IR. *D*, 53BP1 foci formation is not required for ATM-dependent phosphorylation of 53BP1 following DNA damage. 53BP1-deficient embryonic cells were transiently transfected with HA-tagged full-length 53BP1 or a deletion mutant lacking part of the focus formation region. 53BP1 localization and ATM-dependent phosphorylation was analyzed 1 h after 1 Gy of IR by co-staining with anti-HA antibody and anti-phospho-53BP1 antiserum (anti-25P/29P). *E*, an aliquot of the transfected cells was either mock-treated or irradiated with 10 Gy. 53BP1 was immunoprecipitated from cell lysates, and phosphorylation of 53BP1 was analyzed by immunoblotting with the 53BP1 phosphospecific anti-S25P/29P antibodies. *wt*, wild type; *IP*, immunoprecipitation.

DISCUSSION

Upon exposure of cells to genotoxic stress, 53BP1 rapidly redistributes from a pan-nuclear localization to distinct nuclear foci at the sites of DNA strand breaks. In this study we have mapped the region required for 53BP1 foci formation and examined the role of H2AX in 53BP1 accumulation. Moreover, we provided evidence that phosphorylation of 53BP1 by the ATM kinase occurs independently of 53BP1 foci formation.

53BP1 had been speculated to be involved in the DNA damage response based on its C-terminal tandem BRCT domains. This motif was first detected in the BRCA1 C terminus and has been reported to bind directly to DNA breaks (20). Surprisingly the BRCT domains of 53BP1 were found to be dispensable for 53BP1 foci formation. Instead a region upstream of the BRCT motifs proved to be essential for 53BP1 accumulation at sites of DNA strand breaks. Our data suggest that the damage-induced phosphorylation of H2AX directs 53BP1 accumulation at sites of DNA strand breaks. First, H2AX-deficient cells reconstituted with a H2AX phosphomutant failed to induce or sustain 53BP1 foci formation. Second, a 53BP1 fragment (residues 956–1354) contained within the 53BP1 focus localization region interacted strongly with phosphorylated H2AX *in vitro*. Third, 53BP1 co-immunoprecipitates with H2AX in a DNA damage-dependent manner (3). Thus, it is likely that the DNA damage-induced phosphorylation of H2AX at Ser-140 increases the interaction between H2AX and 53BP1 and leads to the accumulation of 53BP1 at the sites of DNA breaks.

Interestingly the focus localization region we mapped includes a region required for 53BP1 kinetochore localization in mitotic cells (residues 1220–1601) (19). Very recently, Morales and colleagues (21) showed that the kinetochore localization region is also essential for 53BP1 foci formation in response to DNA damage suggesting that both events might be regulated in a similar fashion. However, the kinetochore localization of 53BP1 is unlikely to involve DNA lesions (19). We have shown that 53BP1 kinetochore localization appears normal in H2AX-deficient cells, suggesting that kinetochore localization of 53BP1 is not mediated by phospho-H2AX. Further fine mapping studies will be necessary to clarify whether the same 53BP1 region initiates the recruitment of 53BP1 to DNA strand breaks or the kinetochore, respectively.

Phosphorylation by the ATM kinase plays a key role in the activation of various proteins involved in the DNA damage response (for example, see Ref. 22). A recent study by Bakkenist and Kastan (23) revealed that ATM forms an inactive oligomer in unirradiated cells. Upon radiation, ATM is rapidly autophosphorylated and dissociates from the complex thereby providing other substrates access to its kinase domain. Interestingly autophoshorylation and activation of ATM seem to occur at some distance to DNA break sites, and ATM then migrates in the nucleus to phosphorylate various substrates either at the break sites or elsewhere in the nucleus (23). This model is consistent with our finding that ATM-dependent phosphorylation of 53BP1 is not restricted to sites of DNA strand breaks and can occur within the entire nucleus. However, phosphorylation of 53BP1 alone is unlikely to trigger 53BP1 activation since deletion of the ATM target sites does not affect 53BP1 relocalization. Moreover the relocalization of 53BP1 appears to be required for efficient phosphorylation of ATM substrates at the sites of DNA breaks (data not shown). We therefore speculate that the rapid recruitment of 53BP1 to DNA break sites and the retention of 53BP1 at the sites of DNA breaks by binding to phospho-H2AX is one of the key steps in the activation of 53BP1 following DNA damage.

Acknowledgments—We thank Dr. Craig Bassing for the $H2AX^{Flox/Flox}$ and $H2AX^{\Delta/\Delta}$ ES cells. We also thank Drs. Larry Karnitz and Scott Kaufmann and members of the Chen and Karnitz laboratories for helpful discussions. We are grateful to the Mayo Protein Core facility for the synthesis of peptides and to the Mayo Gene Targeted Mouse Core facility for help with the generation of 53BP1-deficient mice and 53BP1-deficient ES cells.

REFERENCES

1. Iwabuchi, K., Bartel, P. L., Li, B., Marraccino, R., and Fields, S. (1994) *Proc. Natl. Acad. Sci. U. S. A.* **91,** 6098–6102
2. Iwabuchi, K., Li, B., Massa, H. F., Trask, B. J., Date, T., and Fields, S. (1998) *J. Biol. Chem.* **273,** 26061–26068
3. Rappold, I., Iwabuchi, K., Date, T., and Chen, J. (2001) *J. Cell Biol.* **153,** 613–620
4. Schultz, L. B., Chehab, N. H., Malikzay, A., and Halazonetis, T. D. (2000) *J. Cell Biol.* **151,** 1381–1390
5. Xia, Z., Morales, J. C., Dunphy, W. G., and Carpenter, P. B. (2000) *J. Biol. Chem.* **276,** 2708–2718
6. Anderson, L., Henderson, C., and Adachi, Y. (2001) *Mol. Cell. Biol.* **21,** 1719–1729
7. Bork, P., Hofmann, K., Bucher, P., Neuwald, A. F., Altschul, S. F., and Koonin, E. V. (1997) *FASEB J.* **11,** 68–76
8. Callebaut, I., and Mornon, J. P. (1997) *FEBS Lett.* **400,** 25–30
9. Yamane, K., Wu, X., and Chen, J. (2002) *Mol. Cell. Biol.* **22,** 555–566
10. DiTullio, R. A., Mochan, T. A., Venere, M., Bartkova, J., Sehested, M., Bartek, J., and Halazonetis, T. D. (2002) *Nat. Cell Biol.* **4,** 998–1002
11. Wang, B., Matsuoka, S., Carpenter, P. B., and Elledge, S. J. (2002) *Science* **298,** 1435–1438
12. Fernandez-Capetillo, O., Chen, H. T., Celeste, A., Ward, I., Romanienko, P. J., Morales, J. C., Naka, K., Xia, Z., Camerini-Otero, R. D., Motoyama, N., Carpenter, P. B., Bonner, W. M., Chen, J., and Nussenzweig, A. (2002) *Nat. Cell Biol.* **4,** 993–997
13. Ward, I. M., Minn, K., Van Deursen, J., and Chen, J. (2003) *Mol. Cell. Biol.* **23,** 2556–2563
14. Celeste, A., Petersen, S., Romanienko, P. J., Fernandez-Capetillo, O., Chen, H. T., Sedelnikova, O. A., Reina-San-Martin, B., Coppola, V., Meffre, E., Difilippantonio, M. J., Redon, C., Pilch, D. R., Olaru, A., Eckhaus, M., Camerini-Otero, R. D., Tessarollo, L., Livak, F., Manova, K., Bonner, W. M., Nussenzweig, M. C., and Nussenzweig, A. (2002) *Science* **296,** 922–927
15. Bassing, C. H., Chua, K. F., Sekiguchi, J., Suh, H., Whitlow, S. R., Fleming, J. C., Monroe, B. C., Ciccone, D. N., Yan, C., Vlasakova, K., Livingston, D. M., Ferguson, D. O., Scully, R., and Alt, F. W. (2002) *Proc. Natl. Acad. Sci. U. S. A.* **99,** 8173–8178
16. Cokol, M., Nair, R., and Rost, B. (2000) *EMBO Rep.* **1,** 411–415
17. Altschul, S. F., Madden, T. L., Schaffer, A. A., Zhang, J., Zhang, Z., Miller, W., and Lipman, D. J. (1997) *Nucleic Acids Res.* **25,** 3389–3402
18. Rogakou, E. P., Pilch, D. R., Orr, A. H., Ivanova, V. S., and Bonner, W. M. (1998) *J. Biol. Chem.* **273,** 5858–5868
19. Jullien, D., Vagnarelli, P., Earnshaw, W. C., and Adachi, Y. (2002) *J. Cell Sci.* **115,** 71–79
20. Yamane, K., Katayama, E., and Tsuruo, T. (2000) *Biochem. Biophys. Res. Commun.* **279,** 678–684
21. Morales, J. C., Xia, Z., Lu, T., Aldrich, M. B., Wang, B., Rosales, C., Kellems, R. E., Hittelman, W. N., Elledge, S. J., and Carpenter, P. B. (2003) *J. Biol. Chem.* **278,** 14971–14977
22. Abraham, R. T. (2001) *Genes Dev.* **15,** 2177–2196
23. Bakkenist, C. J., and Kastan, M. B. (2003) *Nature* **421,** 499–506

MOLECULAR AND CELLULAR BIOLOGY, Apr. 2003, p. 2556–2563 Vol. 23, No. 7
0270-7306/03/$08.00+0 DOI: 10.1128/MCB.23.7.2556–2563.2003

p53 Binding Protein 53BP1 Is Required for DNA Damage Responses and Tumor Suppression in Mice

Irene M. Ward,[1] Kay Minn,[1] Jan van Deursen,[2] and Junjie Chen[1]*

Departments of Oncology[1] and Pediatric and Adolescent Medicine,[2] Mayo Clinic and Foundation, Rochester, Minnesota 55905

Received 19 November 2002/Returned for modification 14 December 2002/Accepted 7 January 2003

53BP1 is a p53 binding protein of unknown function that binds to the central DNA-binding domain of p53. It relocates to the sites of DNA strand breaks in response to DNA damage and is a putative substrate of the ataxia telangiectasia-mutated (ATM) kinase. To study the biological role of 53BP1, we disrupted the 53BP1 gene in the mouse. We show that, similar to ATM$^{-/-}$ mice, 53BP1-deficient mice were growth retarded, immune deficient, radiation sensitive, and cancer prone. 53BP1$^{-/-}$ cells show a slight S-phase checkpoint defect and prolonged G_2/M arrest after treatment with ionizing radiation. Moreover, 53BP1$^{-/-}$ cells feature a defective DNA damage response with impaired Chk2 activation. These data indicate that 53BP1 acts downstream of ATM and upstream of Chk2 in the DNA damage response pathway and is involved in tumor suppression.

Defects in DNA damage recognition and repair mechanisms are associated with cancer predisposition. The tumor suppressor protein p53, a sequence specific transcription factor, plays a central role in the response of mammalian cells to genotoxic stress. 53BP1 (p53 binding protein 1) was cloned as a protein that interacts with the DNA-binding domain of p53 (13). It contains a tandem BRCT (BRCA1 C terminus) motif (5) with sequence homology to the tumor suppressor BRCA1 and DNA damage checkpoint protein scRad9. 53BP1 binds through the first of its C-terminal BRCT repeats and the inter-BRCT linker region to the central DNA-binding domain of p53 (7, 15) and has been shown to enhance p53-mediated transcription of reporter genes (14). More recently, in vitro studies suggest that 53BP1 participates in the cellular response to DNA damage. 53BP1 relocates to multiple nuclear foci within minutes after exposure of cells to ionizing radiation (IR) (2, 22, 23, 28). These foci colocalize with known DNA damage response proteins such as phosphorylated H2AX, Rad50/Mre11/NBS1, BRCA1, and Rad51 at sites of DNA lesions (2, 22, 23). 53BP1 becomes hyperphosphorylated in response to IR, and several lines of evidence suggest that 53BP1 is a downstream target of the ataxia telangiectasia-mutated (ATM) kinase, the product of the gene mutated in ataxia telangiectasia (2, 22, 28). Furthermore, 53BP1 localizes to kinetochores in mitotic cells, suggesting a potential function of 53BP1 in mitotic checkpoint signaling (16).

To study the biological function of 53BP1 in mammals, we created 53BP1-deficient mice. We report here that mice lacking 53BP1 are viable and display a phenotype that partially overlaps with that of ATM-deficient mice. 53BP1-deficient mice are growth retarded, immune deficient, radiation sensitive, and cancer prone. Thus, 53BP1 is required for an appropriate cellular response to DNA damage in vivo.

* Corresponding author. Mailing address: Department of Oncology, Mayo Clinic and Foundation, Rm. 1306, Guggenheim Bldg., 200 First St., SW, Rochester, MN 55905. Phone: (507) 538-1545. Fax: (507) 284-3906. E-mail: chen.junjie@mayo.edu.

MATERIALS AND METHODS

Gene targeting and generation of 53BP1-deficient mice. A mouse 53BP1 cDNA fragment was used as a probe to isolate 53BP1 mouse genomic DNA from a mouse 129 genomic DNA phage library (Stratagene). The genomic DNA was cloned into pZErO-2 (Invitrogen), and the exon-intron structure characterized by restriction digestion, Southern blotting, and DNA sequencing. The targeting vector was constructed by replacing the exon spanning nucleotides 3777 to 4048 of the mouse 53BP1 gene with the PGK-neo^r gene. The targeting vector was linearized and electroporated into 129/SvE embryonic stem (ES) cells. About 200 G418-resistant ES clones were screened by Southern blot analysis by using a probe that hybridizes to a 9.8-kb *Eco*RI restriction fragment in wild-type cells and an 8.3-kb fragment in homologous recombinants. Three independent ES clones with homologous integration at the targeting site were injected into C57BL/6 blastocysts to generate chimeric mice. These chimeras were subsequently crossed with C57BL/6 females, and heterozygous mice with successful germ line transmission of the targeted allele were used to generate 53BP1$^{-/-}$ mice.

Generation of 53BP1$^{-/-}$ MEFs and embryonic cells. Primary mouse embryonic fibroblasts (MEFs) were obtained from e14.5 embryos by a standard procedure. To generate 53BP1$^{-/-}$ embryonic cells, day 3 blastocytes from −/− matings were isolated and an embryonic cell line was established by a standard procedure.

Proliferation and clonogenic assays. MEFs from three 53BP1$^{-/-}$ and three genetically matched 53BP1$^{+/+}$ embryos were plated at a density of 10^5 cells/well in six-well plates. Every day one set of cells was treated with trypsin and counted. At days 3 and 6, cells were split and replated into larger dishes. For the clonognic cell survival assay, 53BP1$^{-/-}$ and 53BP1$^{+/+}$ embryonic cells were plated into 60-by-15-mm dishes and 6 h later exposed to different doses of IR. After 7 days of culture, the number of colonies was counted.

Western blot and immunofluorescence analysis. Western blot analyses were performed by a standard procedure. Immunofluorescence staining was performed as described previously (26). Antibodies against 53BP1, Chk2, Chk2T68P, and γ-H2AX were generated as described previously (22, 26, 27). The antibodies to p53 (FL393G) and actin were purchased from Santa Cruz and Sigma, respectively. The antibodies to mouse NBS1 and BRCA1 were gifts from A. Nussenzweig and L. Chodosh, respectively.

Cell cycle checkpoints and flow cytometry analysis. For analysis of G_2/M checkpoint function, MEFs from 53BP1$^{-/-}$ and genetically matched 53BP1$^{+/+}$ embryos, as well as ES cells, were irradiated with different doses of IR and stained 1 h later with anti-P-Histone 3 (Upstate). Aliquots of the cells were also labeled with bromodeoxyuridine (BrdU) for 1 h before exposure to 6 Gy of IR, harvested at different time points after IR, and stained with anti-BrdU-FITC (Becton Dickinson) and propidium iodide. To monitor radiation-induced inhibition of DNA synthesis, MEFs were labeled for 48 h with 20 nCi of [^{14}C]thymidine ml^{-1} before exposure to 0 or 20 Gy of IR. At 30 min after IR cells were pulse-labeled for 30 min with 2.5 mCi of [^{3}H]thymidine ml^{-1} and harvested. Radioactivity was measured in a liquid scintillation counter.

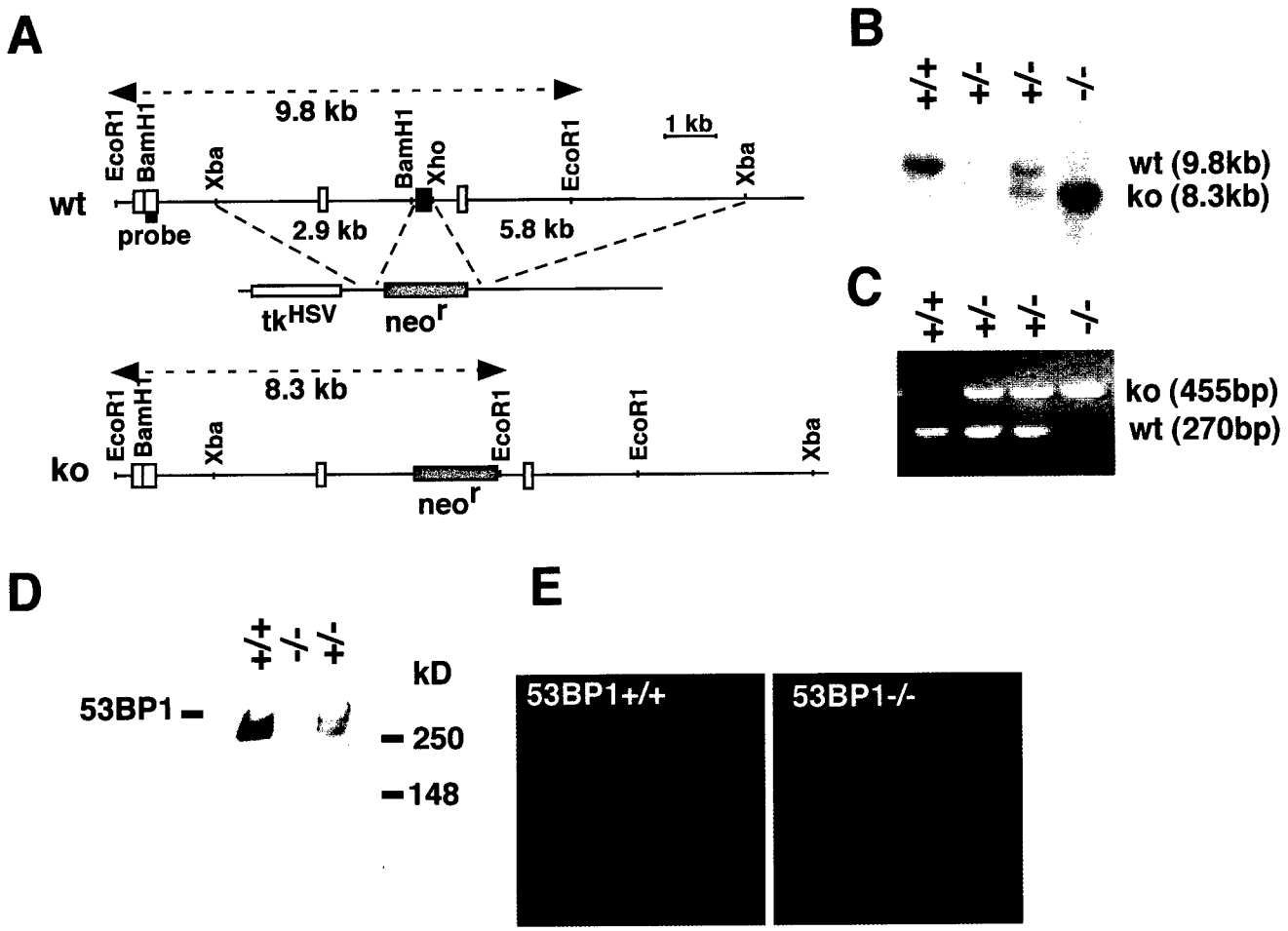

FIG. 1. Targeted disruption of the mouse 53BP1 gene. (A) Map of the genomic locus surrounding the targeted exon, the targeting vector containing the PGK-neo cassette, and the targeted locus. A 5′-flanking probe used for screening ES cell clones and mice is indicated. (B) Southern blot analysis of *Eco*RI-digested genomic DNA. (C) Multiplex PCR genotype analysis with a primer pair for the *neo* gene (resulting in a 455-bp product) and a 5′ external exon (resulting in a 270-bp product). (D) Western blot of cell extracts from mouse testes with an antibody specific for the N terminus of 53BP1. (E) Immunofluorescence analysis of irradiated (1 Gy) 53BP1$^{+/+}$ and 53BP1$^{-/-}$ MEFs with polyclonal antibodies raised against the N terminus of 53BP1.

Thymocytes, white blood cells, and tumor cells were stained with anti-CD4-phycoerythrin and anti-CD8-fluorescein isothiocyanate or the respective isotype controls (all from Pharmingen) and then analyzed on a flow cytometer.

Histopathological analysis and chromosome spreads. Tissues were collected and fixed in 10% buffered formalin or Bouin's fixative, embedded in paraffin blocks, sectioned, and stained with hematoxylin-eosin. Metaphase spreads were prepared by a standard procedure.

RESULTS

Phenotype of 53BP1-deficient mice. To analyze the physiological role of 53BP1 in mammalian cells, we generated 53BP1-deficient mice. The targeting vector was constructed by replacing the exon spanning nucleotides 3777 to 4048 of the mouse 53BP1 cDNA with the PGK-neo^r gene (Fig. 1A to C). 53BP1$^{-/-}$ mice were viable and born at ratios close to the expected Mendelian proportion (25% [+/+], 52% [+/−], and 23% [−/−]). The complete absence of 53BP1 protein was confirmed by Western blot and immunofluorescence analyses with antibodies raised against the N terminus of 53BP1 (Fig. 1D and E).

Since 53BP1 is a putative substrate of ATM in the DNA damage response pathway, we examined whether 53BP1$^{-/-}$ mice show a similar phenotype as ATM-deficient mice. ATM$^{-/-}$ mice are growth retarded and ATM-deficient fibroblasts grow poorly in culture (3, 9, 30). Similarly, 53BP1$^{-/-}$ mice are significantly smaller than their +/+ and +/− littermates (male, 38.29 ± 3.6 g [+/+], 28.28 ± 3.5 g [−/−], and 34.91 ± 2.6 g [+/−]; female, 29.38 ± 4.8 g [+/+], 23.85 ± 3.1 g [−/−], and 27.89 ± 3.5g [+/−]; also see Fig. 2A). Consistent with this finding, MEFs derived from E14.5 null embryos showed a lower proliferation rate than genetically matched wild-type controls (data not shown). ATM-deficient mice are infertile due to meiotic failure (3, 9, 30). In contrast, both male and female 53BP1-deficient mice were fertile, although the average litter size of 53BP1$^{-/-}$ intercrosses was slightly reduced compared to 53BP1-wild-type intercrosses (data not shown). Histological examination of the testes revealed no overt defect in spermatogenesis, suggesting that 53BP1 plays no apparent role in meiosis.

Cell cycle checkpoint regulation in 53BP1$^{-/-}$ cells. ATM-deficient cells exhibit a defect in the G_2/M checkpoint and do

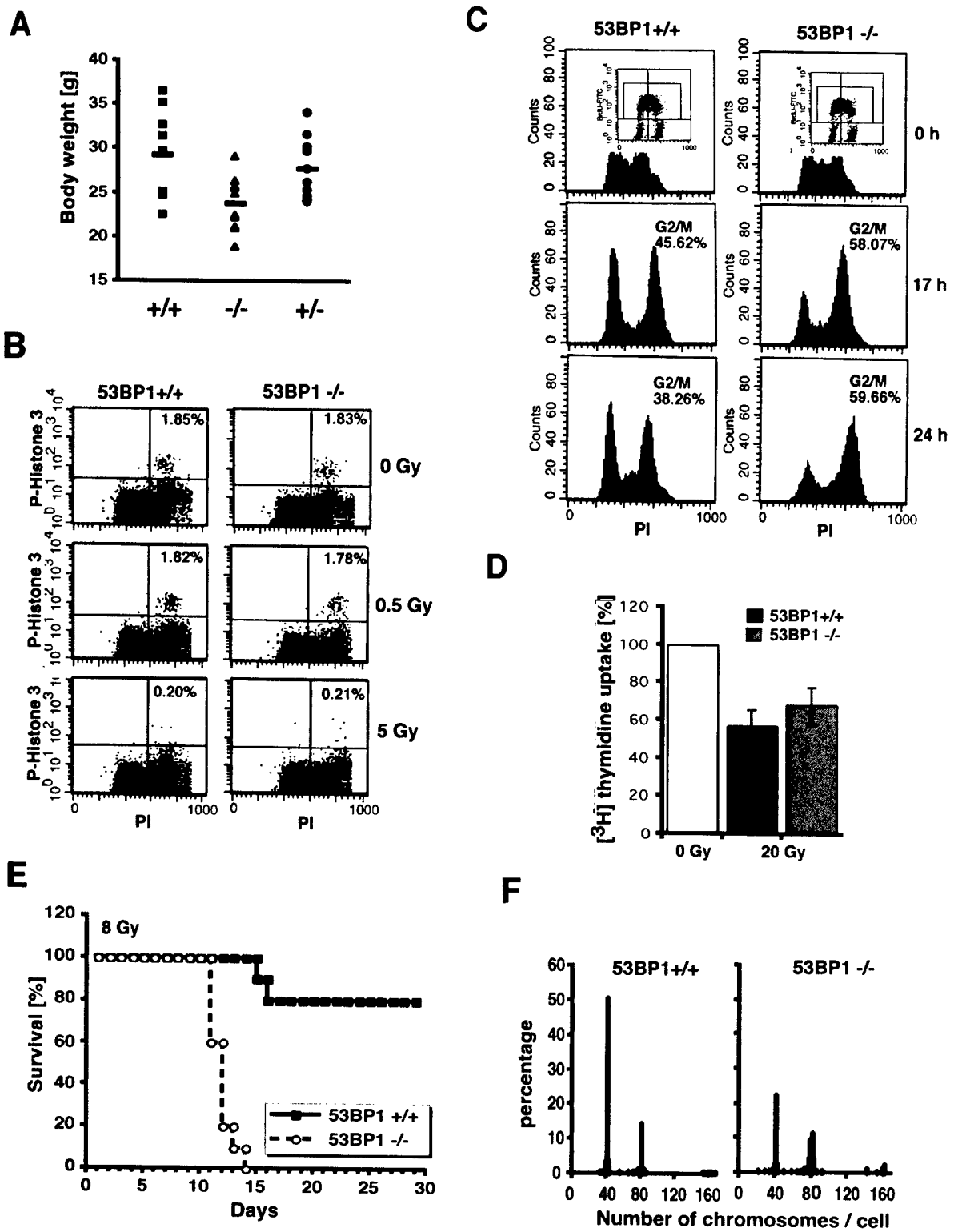

FIG. 2. 53BP1 deficiency results in growth retardation, cell cycle defect, radiosensitivity, and chromosomal instability. (A) Body weights of female 53BP1 wild-type, heterozygous, and knockout mice at 5 months of age. (B) G_2/M arrest of 53BP1$^{+/+}$ and 53BP1$^{-/-}$ embryonic cells in response to 0.5 or 5 Gy of IR. Cells were stained with anti-P-Histone 3 antibody 1 h after IR and analyzed by fluorescence-activated cell sorting. (C) G_2 accumulation of 53BP1$^{+/+}$ and 53BP1$^{-/-}$ MEFs several hours after IR. Cells were pulse-labeled for 1 h with BrdU before exposure to 6 Gy of IR. The cell cycle profile of BrdU-positive cells was analyzed by staining with propidium iodide. Consistent data were obtained in three independent experiments. (D) IR-induced intra-S-phase checkpoint in 53BP1$^{+/+}$ and 53BP1$^{-/-}$ MEFs. DNA synthesis was assessed by [3H]thymidine incorporation 30 min after exposure to 20 Gy of IR. (E) Sensitivity of 10 pairs of female 53BP1$^{-/-}$ and 53BP1$^{+/+}$ littermates to 8 Gy of whole body IR. Similar results were observed with 10 male pairs. (F) Chromosomal instability in 53BP1$^{-/-}$ MEFs. 100 metaphase spreads from genetically matched passage three 53BP1$^{+/+}$ and 53BP1$^{-/-}$ MEFs were analyzed. Consistent data were obtained from three different experiments.

not arrest in G_2 in the first 2 h after IR (for example, see reference 29). However, flow cytometric analysis of phospho-H3-positive mitotic embryonic cells revealed no apparent G_2/M checkpoint defect in 53BP1$^{-/-}$ cells in response to different doses of IR (Fig. 2B and data not shown).

Several hours after IR, ATM-deficient cells show a prolonged accumulation in G_2/M (29). A similar phenotype was observed in 53BP1$^{-/-}$ fibroblasts. As shown in Fig. 2C, irradiated 53BP1-null cells, like 53BP1$^{+/+}$ cells, were arrested in G_2 but showed a delayed exit from the G_2/M phase. Consistent with 53BP1$^{-/-}$ cells arrested at the G_2 phase, the percentage of mitotic cells 24 h after IR was approximately three times lower in nocodazole-treated 53BP1$^{-/-}$ cells than in 53BP1 wild-type cells, as assessed by immunostaining with anti-phospho-histone H3 antibodies (data not shown).

Cells derived from ataxia telangiectasia patients show a defect in the IR-induced G_1 delay (18). In contrast, 53BP1-deficient MEFs, synchronized by a cycle of serum starvation and release, exhibited a normal G_1 arrest in response to 10 to 20 Gy of IR (data not shown).

ATM-deficient cells also feature a defect in the intra-S phase checkpoint, resulting in a radioresistant DNA synthesis phenotype (3). Both 53BP1$^{+/+}$ and 53BP1$^{-/-}$ fibroblasts showed inhibition of DNA synthesis in response to 20 Gy of IR, although the response was slightly impaired in 53BP1$^{-/-}$ cells (Fig. 2D).

Thus, although 53BP1 may play a subtle role in intra-S-phase regulation, it appears not to be critical for G_1 or early G_2/M checkpoint control.

Radiosensitivity of 53BP1$^{-/-}$ mice and cells. Another hallmark of ATM-deficiency is extreme radiation sensitivity (for example, see reference 3). Similarly, 53BP1$^{-/-}$ mice showed a marked hypersensitivity to whole-body irradiation. All 53BP1$^{-/-}$ mice died by 14 days after exposure to 8 Gy of IR, whereas the majority of 53BP1$^{+/+}$ mice were viable for at least 2 months after irradiation (Fig. 2E). Necroptic examination revealed radiation-induced intestinal bleeding and bone marrow failure as the cause of death (data not shown). Consistent with this finding, in vitro clonogenic survival assays with embryonic cells indicated a two- to threefold-higher radiation sensitivity in 53BP1-deficient cells than in 53BP1-wild-type cells, although the difference was less dramatic than in vivo (data not shown).

Chromosomal instability of 53BP1$^{-/-}$ cells. To determine whether loss of 53BP1 causes chromosomal instability, another characteristic of ATM$^{-/-}$ cells, we examined metaphase spreads of passage 3 53BP1$^{-/-}$ and 53BP1$^{+/+}$ MEFs. Unlike ATM-deficient cells, 53BP1$^{-/-}$ fibroblasts showed no spontaneous chromosomal breaks. However, we observed a tendency toward aneuploidy and/or tetraploidy in 53BP1-null cells, suggesting a possible defect in chromosome segregation (Fig. 2F).

Immunodeficiency and thymic lymphomas in 53BP1$^{-/-}$ mice. ATM$^{-/-}$ mice show various immune defects, including reduced numbers of pre-B cells, thymocytes, and peripheral T cells, and develop malignant thymic lymphomas by between 2 and 4 months of age (3, 9, 30). We therefore sought to determine whether the loss of 53BP1 might be accompanied by immunological abnormalities and predisposition to tumor formation. Indeed, thymus cellularity in 53BP1$^{-/-}$ mice was reduced by 40% compared to wild-type littermates. Immunophenotyping of 6-week-old mice revealed an approximately twofold reduction in the percentage of CD4$^+$ mature thymocytes (with absolute average numbers of 7×10^6 cells in 53BP1$^{+/+}$ mice and 2.8×10^6 cells in 53BP1$^{-/-}$ mice) accompanied by a maximum twofold increase in the percentage of CD4$^-$ CD8$^-$ progenitors. CD4$^+$ T lymphocytes in the peripheral blood of 53BP1$^{-/-}$ mice were also reduced by approximately twofold (with absolute average numbers of 8.2×10^5 cells/ml in 53BP1$^{-/-}$ mice and 16.9×10^5 cells/ml in 53BP1$^{+/+}$ mice). Furthermore, of 101 53BP1$^{-/-}$ mice, 8 developed massive thymic lymphomas with or without infiltration of the lymph nodes, spleen, and kidney at the ages of 4 to 7 months (Fig. 3A to C). Flow cytometric analysis of three of these tumors revealed a CD4$^+$ CD8$^+$ immunophenotype (Fig. 3A and data not shown). Although the tumor frequency in 53BP1$^{-/-}$ mice is much lower than in ATM$^{-/-}$ mice (8% versus 100%), it is highly significant since none of the 53BP1$^{+/+}$ and 53BP1$^{+/-}$ mice ($n = 54$ and $n = 97$, respectively) developed any tumors over the same time period. In addition to the eight 53BP1$^{-/-}$ mice with malignant lymphomas, nine more 53BP1$^{-/-}$ mice died at the ages of 1 to 7 months without overt detectable tumors (Fig. 3D). Given the chronic immunosuppression of 53BP1$^{-/-}$ mice, it is possible that some of these deaths might be due to overwhelming opportunistic infections. Among the control animals, only one 53BP1$^{+/+}$ mouse and two 53BP1$^{+/-}$ miced died of unidentified reasons (Fig. 3D).

Role of 53BP1 in DNA damage signaling pathway. The partially overlapping phenotypes of 53BP1- and ATM-deficient mice support the hypothesis that 53BP1 acts downstream of ATM in the DNA damage pathway. ATM becomes activated in response to irradiation and phosphorylates numerous downstream targets, including H2AX, NBS1, Chk2, and p53, that mediate cell cycle checkpoint control and DNA repair (for example, see reference 1). To obtain a better understanding of the complex organization of this pathway, we examined the effect of 53BP1 deficiency on the activation of some of these downstream targets.

We have shown earlier that 53BP1 associates with γ-H2AX within minutes after exposure to IR (22), thus raising the possibility that γ-H2AX may be required for the recruitment of 53BP1. Indeed, 53BP1 foci are not observed in H2AX-deficient cells (6). Consistent with this model, γ-H2AX foci formation was found normal in 53BP1$^{-/-}$ MEFs (Fig. 4A), suggesting that 53BP1 acts downstream of ATM and H2AX. Since H2AX is also required for the localization of NBS1 to the sites of DNA breaks (6, 21), we examined whether any of these events are 53BP1 dependent. As shown in Fig. 4A, radiation-induced NBS1 foci formation appears to be normal in 53BP1$^{-/-}$ cells, suggesting that 53BP1 is not required for the recruitment of NBS1 to sites of DNA strand breaks.

Chk2 is another downstream effector of ATM. Chk2 is activated after IR and contributes to the IR-induced checkpoint control by phosphorylating several substrates including Cdc25C, Cdc25A, BRCA1, and p53 (4). ATM phosphorylates Chk2 at Thr-68 in response to IR, and this phosphorylation event is required for the full activation of Chk2 kinase (19, 20). Coimmunoprecipitation analyses demonstrate an interaction between 53BP1 and Chk2 in undam-

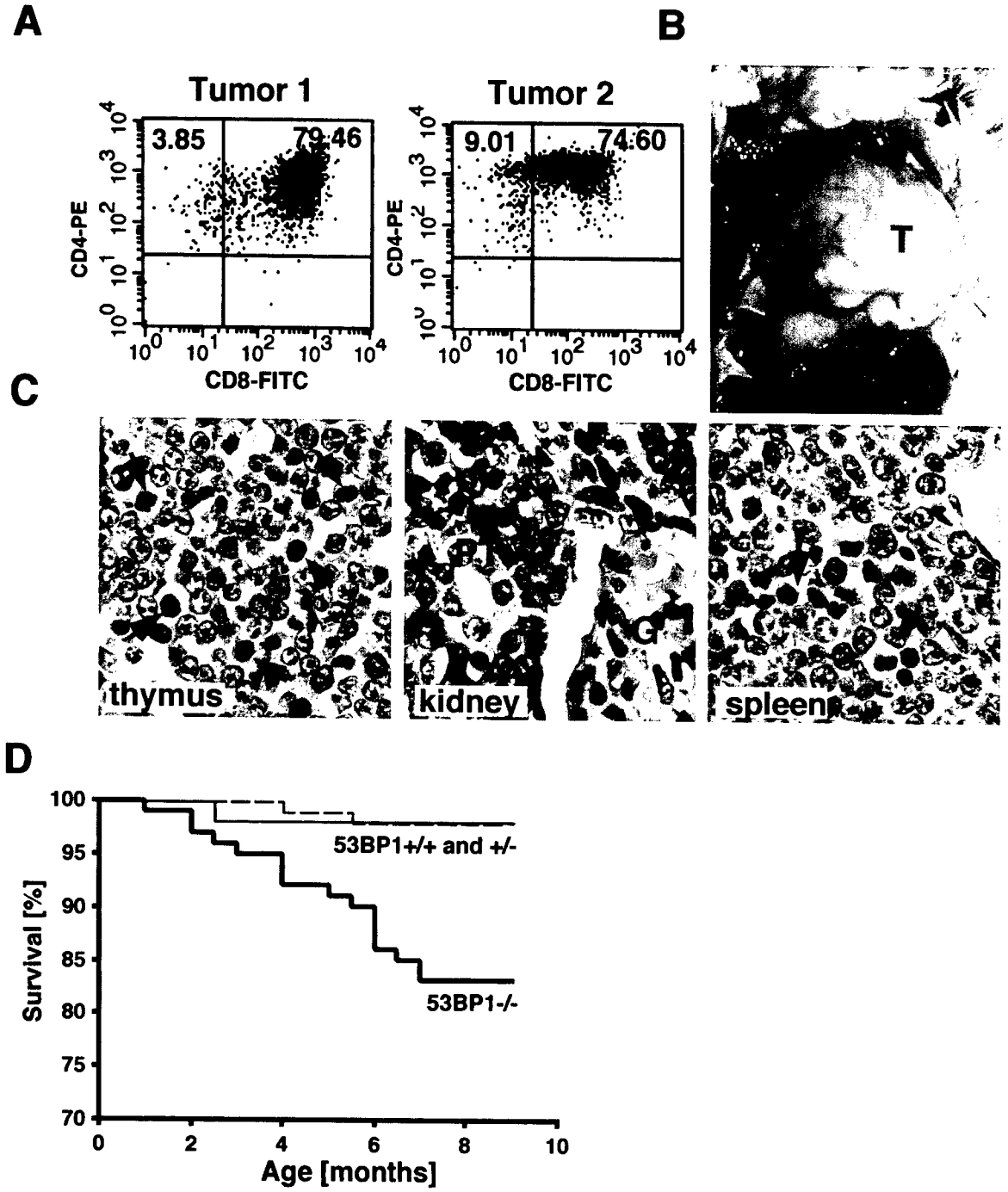

FIG. 3. 53BP1$^{-/-}$ mice are tumor prone. (A) CD4 and CD8 cell surface expression of cells from two different thymic lymphomas was assessed by flow cytometry. (B) Massive thymic lymphoma (T) in a 4-month-old 53BP1$^{-/-}$ mouse. (C) Hematoxylin-and-eosin-stained sections from the thymus, spleen, and kidney of a 53BP1$^{-/-}$ animal with thymic lymphoma. Monomorphic lymphoblastic tumor cells are dominant in all three tissues. The arrows indicate mitotic figures. G, glomerulus; PT, proximal tubulus. (D) Overall survival of 53BP1$^{+/+}$ (n = 54), 53BP1$^{+/-}$ (n = 97), and 53BP1$^{-/-}$ (n = 101) mice over a period of 10 months.

aged cells (Fig. 4B). Interestingly, this interaction decreases after IR (Fig. 4B). Since we have shown earlier that the activated form of Chk2 localizes in distinct foci at the sites of DNA lesions (27), we first examined the focus formation of phospho-Chk2. In these experiments, we used a guinea pig anti-Chk2T68P antibody that specifically recognizes Chk2 in Chk2$^{+/+}$ cells but not in Chk2$^{-/-}$ cells (Fig. 4G). As shown in Fig. 4C, focus formation of phosphorylated Chk2 (Chk2T68P) was abolished in 53BP1$^{-/-}$ MEFs upon exposure to 1 Gy of IR. Furthermore, Chk2 phosphorylation, as assessed by gel mobility shift, was reduced in 53BP1$^{-/-}$ MEFs in response to low doses of radiation (≤5 Gy, Fig. 4E

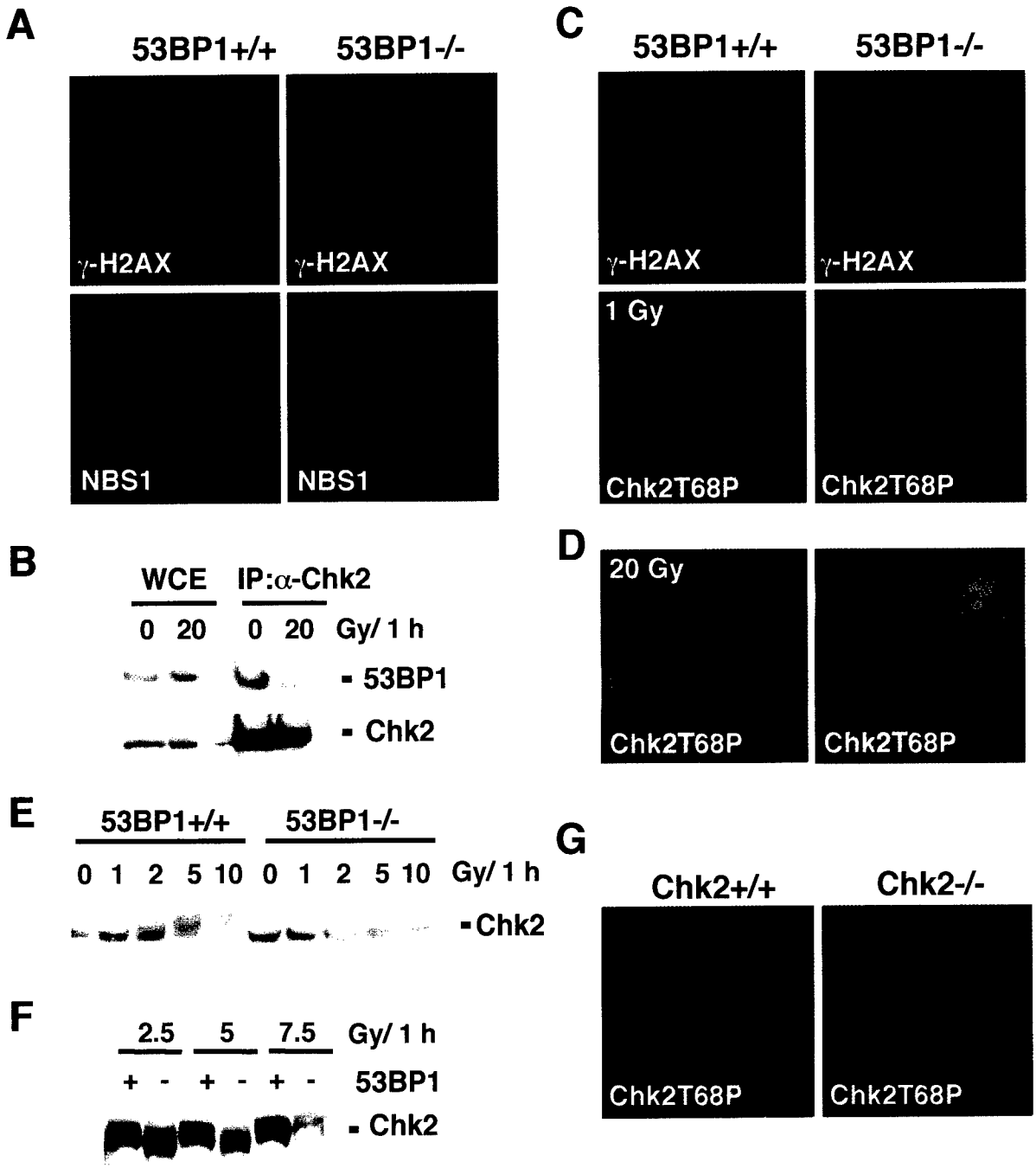

FIG. 4. Irradiated 53BP$^{-/-}$ MEFs show impaired Chk2 activation after low doses of IR. (A) γ-H2AX and NBS1 focus formation 6 h after exposure to 6 Gy of IR is unaffected in 53BP1$^{-/-}$MEFs compared to 53BP1 wild-type MEFs, as assessed by immunofluorescence staining. (B) Coimmunoprecipitation of 53BP1 and Chk2 in untreated or irradiated 293T cells. (C) Activated Chk2 phosphorylated at Thr 68 (Chk2T68) forms foci in 53BP1$^{+/+}$ MEFs 1 h after exposure to 1 Gy of IR. No foci are detectable in 53BP1$^{-/-}$ MEFs at this low dose of IR. γ-H2AX staining is shown as a control. (D) Chk2T68P foci form in both 53BP1$^{+/+}$ and 53BP1$^{-/-}$ cells in response to 20 Gy of IR. (E) Chk2 mobility shift is reduced in 53BP1$^{-/-}$ MEFs in response to low-dose radiation. Cell lysates from 53BP1$^{+/+}$ and 53BP1$^{-/-}$ MEFs were prepared 1 h after IR and immunoblotted with anti-Chk2 antibody. (F) For better comparison of the Chk2 mobility shift, lysates from irradiated 53BP1$^{+/+}$ and 53BP1$^{-/-}$ cells were run side by side. (G) The guinea pig anti-Chk2T68P antibody specifically recognizes Chk2.

and F). However, no difference in Chk2T68 focus formation or Chk2 mobility shift was observed at high doses of IR (Fig. 4D and F and data not shown). These findings suggest that 53BP1 is required for optimal activation of Chk2 after low doses of IR.

DISCUSSION

By disrupting the 53BP1 gene, we generated mice that lack 53BP1 protein. 53BP1-deficient mice are growth retarded, immunocompromised, and highly radiation sensitive. Further-

more, 8 of 101 53BP1$^{-/-}$ mice developed lymphoid tumors at 4 to 7 months of age. Cells derived from 53BP1-deficient mice show a tendency to genetic instability and feature a defective DNA damage response with impaired Chk2 activation. Thus, 53BP1 is likely to be required for the cellular response to DNA damage, although its precise role remains to be resolved.

We did not observe any marked cell cycle checkpoint defects in 53BP1-deficient cells. B cells from 53BP1$^{-/-}$ mice (11), as well as human cell lines treated with small interfering RNA directed against 53BP1, show an impaired early G_2M checkpoint in response to low-dose IR (25). However, we failed to detect this defect in 53BP1$^{-/-}$ mouse embryonic cells. This discrepancy may be due to tissue-specific functions of 53BP1 since the experiments were performed with different types of cells or cell lines. Similarly, H2AX$^{-/-}$ B cells show a clearly impaired early G_2M checkpoint, whereas the defect is very minor in H2AX$^{-/-}$ MEFs (11).

The prolonged G_2 arrest observed several hours after exposure to IR is unlikely to represent a checkpoint defect but rather reflects an impaired ability to repair DNA double-strand breaks (DSBs) prior to progressing through the cell cycle. This idea is supported by the hypersensitivity of 53BP1-deficient mice to IR. Mammalian cells are thought to repair DNA DSBs primarily by nonhomologous end joining (17). Homologous recombination, the predominant DSB repair pathway in bacteria and yeast, appears to have a minor contribution to the repair of IR in adult mice, although it plays a major role during DNA replication in embryos (10). The IR hypersensitivity observed in adult 53BP1$^{-/-}$ mice, together with a moderate IR sensitivity seen in embryonic cells, points to a defect in the DNA end-joining pathway. However, further experiments need to be conducted to resolve the precise repair defects in 53BP1-deficient cells.

One important function of DNA end joining lies in the processing of RAG1/2-induced DSBs that arise during the rearrangement of V(D)J segments in T-cell receptor and immunoglobulin genes (10). Unrepaired RAG-induced DSBs can initiate translocations that lead to oncogenic gene amplification and transformation (8, 31). 53BP1-deficient mice exhibit immunological abnormalities and an increased risk of developing lymphomas. We speculate that 53BP1$^{-/-}$ lymphomas arise from an inability to detect or repair abnormal V(D)J recombination, although further studies are necessary to clarify the underlying mechanism of lymphoma development in 53BP1-deficient mice.

53BP1-deficient cells exhibit a defect in Chk2 activation in response to low-dose IR. Interestingly, the phenotype of Chk2$^{-/-}$ mice is very different from that of 53BP1$^{-/-}$ mice. Chk2-deficient mice show reduced sensitivity to IR, and Chk2$^{-/-}$ thymocytes exhibit resistance to IR-induced apoptosis (12, 24). In contrast, 53BP1$^{-/-}$ mice are IR hypersensitive and 53BP1$^{-/-}$ thymocytes show increased IR-induced apoptosis (unpublished observations). These differences indicate that the phenotype of 53BP1-deficient mice or cells is not primarily mediated by Chk2, although 53BP1 is required for optimal Chk2 activation in response to low-dose IR.

Taken together, our data demonstrate that 53BP1 plays a role early in the DNA damage response pathway. 53BP1 acts downstream of ATM and H2AX and participates in a subset of ATM functions. 53BP1 is required for optimal activation of Chk2 in response to low doses of IR. More importantly, loss of 53BP1 leads to radiation sensitivity and tumorigenesis in mice, further supporting the hypothesis that defects in DNA damage responses contribute to tumorigenesis in mammals.

ACKNOWLEDGMENTS

We thank Andre Nussenzweig, Lewis Chodosh, Xiaohua Wu, Shirdar Ganesan, and David Livingston for valuable reagents and Larry Karnitz, Scott Kaufmann, and members of the Chen and Karnitz laboratories for helpful discussions. We are grateful to the Mayo Protein Core facility for synthesis of peptides and the Mayo Monoclonal Core facility for help in antibody production.

This work was supported by grants from National Institute of Health, the Breast Cancer Research Foundation, and Prospect Creek Foundation. J.C. is a recipient of DOD breast cancer career development award. I.W. is supported by a postdoctoral fellowship from the DOD Breast Cancer Research program.

REFERENCES

1. **Abraham, R. T.** 2001. Cell cycle checkpoint signaling through the ATM and ATR kinases. Genes Dev. **15**:2177–2196.
2. **Anderson, L., C. Henderson, and Y. Adachi.** 2001. Phosphorylation and rapid relocalization of 53BP1 to nuclear foci upon DNA damage. Mol. Cell. Biol. **21**:1719–1729.
3. **Barlow, C., S. Hirotsune, R. Paylor, M. Liyanage, M. Eckhaus, F. Collins, Y. Shiloh, J. N. Crawley, T. Ried, D. Tagle, and A. Wynshaw-Boris.** 1996. ATM-deficient mice: a paradigm of ataxia telangiectasia. Cell **86**:159–171.
4. **Bartek, J., J. Falck, and J. Lukas.** 2001. CHK2 kinase: a busy messenger. Nat. Rev. Mol. Cell. Biol. **2**:877–886.
5. **Callebaut, I., and J. P. Mornon.** 1997. From BRCA1 to RAP1: a widespread BRCT module closely associated with DNA repair. FEBS Lett. **400**:25–30.
6. **Celeste, A., S. Petersen, P. J. Romanienko, O. Fernandez-Capetillo, H. T. Chen, O. A. Sedelnikova, B. Reina-San-Martin, V. Coppola, E. Meffre, M. J. Difilippantonio, C. Redon, D. R. Pilch, A. Olaru, M. Eckhaus, R. D. Camerini-Otero, L. Tessarollo, F. Livak, K. Manova, W. M. Bonner, M. C. Nussenzweig, and A. Nussenzweig.** 2002. Genomic instability in mice lacking histone H2AX. Science **296**:922–927.
7. **Derbyshire, D. J., B. P. Basu, L. C. Serpell, W. S. Joo, T. Date, K. Iwabuchi, and A. J. Doherty.** 2002. Crystal structure of human 53BP1 BRCT domains bound to p53 tumour suppressor. EMBO J. **21**:3863–3872.
8. **Difilippantonio, M. J., S. Petersen, H. T. Chen, R. Johnson, M. Jasin, R. Kanaar, T. Ried, and A. Nussenzweig.** 2002. Evidence for replicative repair of DNA double-strand breaks leading to oncogenic translocation and gene amplification. J. Exp. Med. **196**:469–480.
9. **Elson, A., Y. Wang, C. J. Daugherty, C. C. Morton, F. Zhou, J. Campos-Torres, and P. Leder.** 1996. Pleiotropic defects in ataxia-telangiectasia protein-deficient mice. Proc. Natl. Acad. Sci. USA **93**:13084–13089.
10. **Essers, J., H. van Steeg, J. de Wit, S. M. Swagemakers, M. Vermeij, J. H. Hoeijmakers, and R. Kanaar.** 2000. Homologous and non-homologous recombination differentially affect DNA damage repair in mice. EMBO J. **19**:1703–1710.
11. **Fernandez-Capetillo, O., H. T. Chen, A. Celeste, I. Ward, P. J. Romanienko, J. C. Morales, K. Naka, Z. Xia, R. D. Camerini-Otero, N. Motoyama, P. B. Carpenter, W. M. Bonner, J. Chen, and A. Nussenzweig.** 2002. DNA damage-induced G_2-M checkpoint activation by histone H2AX and 53BP1. Nat. Cell Biol. **4**:993–997.
12. **Hirao, A., A. Cheung, G. Duncan, P. M. Girard, A. J. Elia, A. Wakeham, H. Okada, T. Sarkissian, J. A. Wong, T. Sakai, E. De Stanchina, R. G. Bristow, T. Suda, S. W. Lowe, P. A. Jeggo, S. J. Elledge, and T. W. Mak.** 2002. Chk2 is a tumor suppressor that regulates apoptosis in both an ataxia telangiectasia mutated (ATM)-dependent and an ATM-independent manner. Mol. Cell. Biol. **22**:6521–6532.
13. **Iwabuchi, K., P. L. Bartel, B. Li, R. Marraccino, and S. Fields.** 1994. Two cellular proteins that bind to wild-type but not mutant p53. Proc. Natl. Acad. Sci. USA **91**:6098–6102.
14. **Iwabuchi, K., B. Li, H. F. Massa, B. J. Trask, T. Date, and S. Fields.** 1998. Stimulation of p53-mediated transcriptional activation by the p53-binding proteins, 53BP1 and 53BP2. J. Biol. Chem. **273**:26061–26068.
15. **Joo, W. S., P. D. Jeffrey, S. B. Cantor, M. S. Finnin, D. M. Livingston, and N. P. Pavletich.** 2002. Structure of the 53BP1 BRCT region bound to p53 and its comparison to the Brca1 BRCT structure. Genes Dev. **16**:583–593.
16. **Jullien, D., P. Vagnarelli, W. C. Earnshaw, and Y. Adachi.** 2002. Kinetochore localisation of the DNA damage response component 53BP1 during mitosis. J. Cell Sci. **115**:71–79.
17. **Kanaar, R., J. H. Hoeijmakers, and D. C. van Gent.** 1998. Molecular mechanisms of DNA double strand break repair. Trends Cell Biol. **8**:483–489.
18. **Khanna, K. K., H. Beamish, J. Yan, K. Hobson, R. Williams, I. Dunn, and**

M. F. Lavin. 1995. Nature of G_1/S cell cycle checkpoint defect in ataxia-telangiectasia. Oncogene **11:**609–618.

19. **Matsuoka, S., G. Rotman, A. Ogawa, Y. Shiloh, K. Tamai, and S. J. Elledge.** 2000. Ataxia telangiectasia-mutated phosphorylates Chk2 in vivo and in vitro. Proc. Natl. Acad. Sci. USA **97:**10389–10394.
20. **Melchionna, R., X. B. Chen, A. Blasina, and C. H. McGowan.** 2000. Threonine 68 is required for radiation-induced phosphorylation and activation of Cds1. Nat. Cell Biol. **2:**762–765.
21. **Paull, T. T., E. P. Rogakou, V. Yamazaki, C. U. Kirchgessner, M. Gellert, and W. M. Bonner.** 2000. A critical role for histone H2AX in recruitment of repair factors to nuclear foci after DNA damage. Curr. Biol. **10:**886–895.
22. **Rappold, I., K. Iwabuchi, T. Date, and J. Chen.** 2001. Tumor suppressor p53 binding protein 1 (53BP1) is involved in DNA damage-signaling pathways. J. Cell Biol. **153:**613–620.
23. **Schultz, L. B., N. H. Chehab, A. Malikzay, and T. D. Halazonetis.** 2000. p53 binding protein 1 (53BP1) is an early participant in the cellular response to DNA double-strand breaks. J. Cell Biol. **151:**1381–1390.
24. **Takai, H., K. Naka, Y. Okada, M. Watanabe, N. Harada, S. Saito, C. W. Anderson, E. Appella, M. Nakanishi, H. Suzuki, K. Nagashima, H. Sawa, K. Ikeda, and N. Motoyama.** 2002. Chk2-deficient mice exhibit radioresistance and defective p53-mediated transcription. EMBO J. **21:**5195–5205.
25. **Wang, B., S. Matsuoka, P. B. Carpenter, and S. J. Elledge.** 2002. 53BP1, a mediator of the DNA damage checkpoint. Science **283:**1435–1438.
26. **Ward, I. M., and J. Chen.** 2001. Histone H2AX is phosphorylated in an ATR-dependent manner in response to replicational stress. J. Biol. Chem. **276:**47759–47762.
27. **Ward, I. M., X. Wu, and J. Chen.** 2001. Threonine 68 of Chk2 is phosphorylated at sites of DNA strand breaks. J. Biol. Chem. **276:**47755–47758.
28. **Xia, Z., J. C. Morales, W. G. Dunphy, and P. B. Carpenter.** 2001. Negative cell cycle regulation and DNA damage inducible phosphorylation of the BRCT protein 53BP1. J. Biol. Chem. **276:**2708–2718.
29. **Xu, B., S. T. Kim, D. S. Lim, and M. B. Kastan.** 2002. Two molecularly distinct G_2/M checkpoints are induced by ionizing irradiation. Mol. Cell. Biol. **22:**1049–1059.
30. **Xu, Y., T. Ashley, E. E. Brainerd, R. T. Bronson, M. S. Meyn, and D. Baltimore.** 1996. Targeted disruption of ATM leads to growth retardation, chromosomal fragmentation during meiosis, immune defects, and thymic lymphoma. Genes Dev. **10:**2411–2422.
31. **Zhu, C., K. D. Mills, D. O. Ferguson, C. Lee, J. Manis, J. Fleming, Y. Gao, C. C. Morton, and F. W. Alt.** 2002. Unrepaired DNA breaks in p53-deficient cells lead to oncogenic gene amplification subsequent to translocations. Cell **109:**811–821.